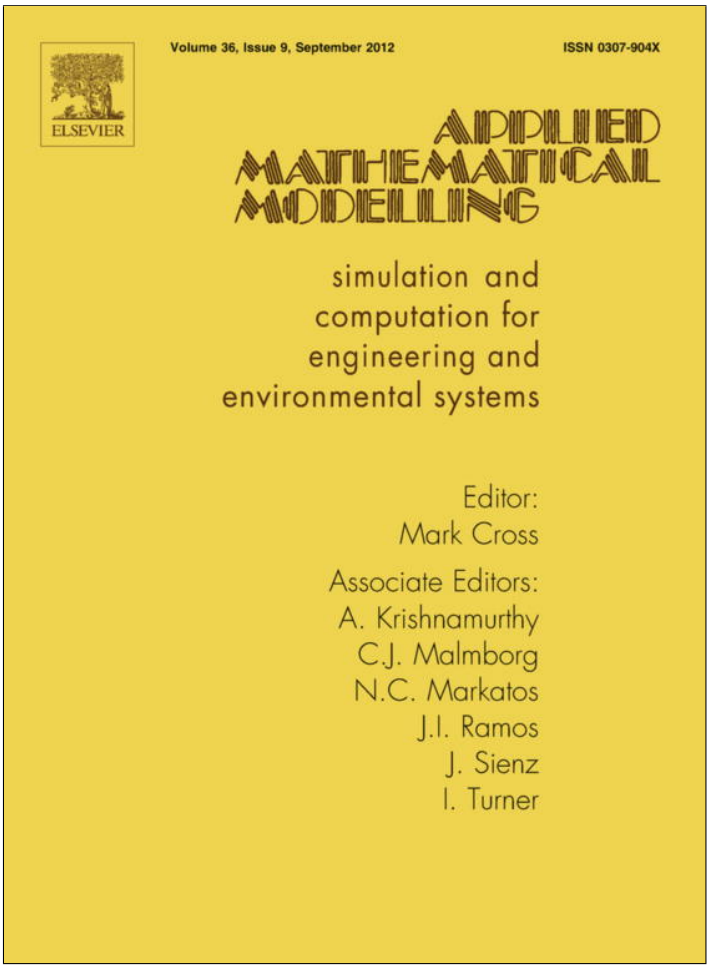

Applied Mathematical Modelling 36 (2012) 3949–3970

Contents lists available at SciVerse ScienceDirect

Applied Mathematical Modelling

journal homepage: www.elsevier.com/locate/apm

MHD oblique stagnation-point flow of a micropolar fluid

Alessandra Borrelli *, Giulia Giantesio, Maria Cristina Patria

Dipartimento di Matematica, Università di Ferrara, via Machiavelli 35, 44100 Ferrara, Italy

ARTICLE INFO

Article history:
Received 14 January 2011
Received in revised form 17 October 2011
Accepted 2 November 2011
Available online 17 November 2011

Keywords:
Micropolar fluids
MHD flow
Oblique stagnation-point flow

ABSTRACT

The steady two-dimensional oblique stagnation-point flow of an electrically conducting micropolar fluid in the presence of a uniform external electromagnetic field ($\mathbf{E}_0, \mathbf{H}_0$) is analysed and some physical situations are examined. In particular, if $\mathbf{E}_0$ vanishes, $\mathbf{H}_0$ lies in the plane of the flow, with a direction not parallel to the boundary, and the induced magnetic field is neglected, it is proved that the oblique stagnation-point flow exists if, and only if, the external magnetic field is parallel to the dividing streamline. In all cases it is shown that the governing nonlinear partial differential equations admit similarity solutions and the resulting ordinary differential problems are solved numerically. Finally, the behaviour of the flow near the boundary is analysed; this depends on the three dimensionless material parameters, and also on the Hartmann number if $\mathbf{H}_0$ is parallel to the dividing streamline.

1. Introduction

The micropolar fluids introduced by Eringen [1] physically represent fluids consisting of rigid randomly oriented particles suspended in a viscous medium which have an intrinsic rotational micromotion (for example biological fluids in thin vessels, polymeric suspensions, slurries, colloidal fluids). Extensive reviews of the theory and its applications can be found in [2,3].

The aim of this paper is to study how the steady two dimensional oblique stagnation-point flow of an electrically conducting micropolar fluid is influenced by a uniform external electromagnetic field ($\mathbf{E}_0, \mathbf{H}_0$). The motions we find depend upon how the applied electromagnetic field is oriented relative to the flat boundary.

Oblique stagnation-point flow appears when a jet of fluid impinges obliquely on a rigid wall at an arbitrary angle of incidence. From a mathematical point of view, such a flow is obtained by combining orthogonal stagnation-point flow with a shear flow parallel to the wall. The steady two-dimensional oblique stagnation-point flow of a Newtonian fluid has been object of many investigations starting from the paper of Stuart in 1959 [4]. We refer to [5,6] for a review.

The orthogonal plane and axially symmetric stagnation-point flow of a micropolar fluid have been treated by Guram and Smith [7], who reduced the equations to dimensionless form, including three dimensionless parameters and integrated them numerically. Previously Ahmadi [8] obtained self-similar solutions of the boundary layer equations for micropolar flow imposing restrictive conditions on the material parameters which make the equations to contain only one parameter. This restrictive approach has been followed in [9,10] in order to study the oblique stagnation-point flow in the absence of an external electromagnetic field. Moreover this restrictive approach has been followed also in [11–13] in order to study the orthogonal stagnation-point flow in the presence of an external electromagnetic field for some different physical conditions.

* Corresponding author.
E-mail addresses: brs@unife.it (A. Borrelli), gntgli@unife.it (G. Giantesio), pat@unife.it (M.C. Patria).

0307-904X/$ - see front matter © 2011 Elsevier Inc. All rights reserved.
doi:10.1016/j.apm.2011.11.004

In this paper we extend the results of [14] about Newtonian fluids to incompressible homogeneous micropolar fluids avoiding the previous restrictive conditions on the material parameters, assuming potential flow far from the boundary and prescribing the strict adherence condition on the flat plane boundary.

First of all, we summarize the results of [14] concerning an inviscid fluid, and analyse three cases, which are significant from a physical point of view. In the first two cases, an external constant field, either electric or magnetic, is impressed parallel to the rigid wall. In both cases, we have found that an oblique stagnation-point flow exists, and we determined the exact induced magnetic field. In the third case, we suppose that $\mathbf{E}_0$ vanishes and $\mathbf{H}_0$ lies in the plane of the flow, with a direction not parallel to the boundary. Under the hypothesis that the magnetic Reynolds number is small, we neglect the induced magnetic field, as it is customary in the literature. We have proved that the oblique stagnation-point flow exists if, and only if, $\mathbf{H}_0$ is parallel to the dividing streamline.

Then we consider the same problems for a micropolar fluid, assuming that at infinity, the velocity $\mathbf{v}$ approaches the flow of an inviscid fluid for which the stagnation-point is shifted from the origin [6,15–17], and the microrotation $\mathbf{w}$ is given by $\mathbf{w} = \frac{1}{2}\nabla \times \mathbf{v}$, i.e. the micropolar fluid behaves like a classical fluid far from the wall. The coordinates of this stagnation-point contain two constants: A and B. A is determined as part of the solution of the orthogonal flow, and B is free.

As far as the velocity and the microrotation are concerned, in the first two cases we find the same equations of the oblique stagnation-point flow in the absence of an electromagnetic field, while the induced magnetic field is obtained by direct integration. Hence, the external uniform electromagnetic field does not influence the flow, and modifies only the pressure p. Moreover ∇p has a constant component parallel to the wall proportional to $B - A$. This does not appear in the orthogonal stagnation-point flow. This component determines the displacement parallel to the boundary of the uniform shear flow. The flow is obtained for different values of B and of the material parameters by numerical integration using the MATLAB finite difference code **bvp4c** [18].

We remark that the influence of the viscosity appears only in a layer lining the boundary whose thickness is larger than that in the orthogonal stagnation-point flow.

Finally, in the more general case in which $\mathbf{H}_0$ is parallel to the dividing streamline of the inviscid flow, we find that the flow has to satisfy an ordinary differential problem whose solution depend on $\mathbf{H}_0$ through the Hartmann number M. The numerical integration is provided using the MATLAB routine **bvp4c**. In this case, A (and so the stagnation-point) depends on M and decreases as M is increased. Further, when the material parameters are fixed, the influence of the viscosity appears only in a layer near to the wall depending on M whose thickness decreases as M increases from zero. This is standard in magnetohydrodynamics.

Some numerical examples and pictures are given in order to illustrate the effects due to the magnetic field.

The paper is organized in this way:

In Section 2, we summarize the results in [14] for an inviscid fluid.

Section 3 is devoted to treat the same physical problems for a micropolar fluid. Theorems 4, 6, 7 collect our results.

Further, we study the behaviour of the flow near the wall. We show that it depends on the three dimensionless material parameters, and also on the Hartmann number in the third case.

In Section 4, we numerically integrate the previous problems, and discuss some numerical results.

2. Inviscid fluids

Consider the MHD steady plane stagnation-point flow of an inviscid, homogeneous, incompressible, electrically conducting fluid filling the region $\mathcal{S}$, given by

$$\mathcal{S} = \{\mathbf{x} \in \mathbb{R}^3 : (x_1, x_3) \in \mathbb{R}^2, x_2 > 0\}. \tag{1}$$

The boundary of $\mathcal{S}$ is a rigid, fixed, non-electrically conducting wall.

The equations governing such a flow in the absence of external mechanical body forces are:

$$\begin{aligned} &\rho \mathbf{v} \cdot \nabla \mathbf{v} = -\nabla p + \mu_e (\nabla \times \mathbf{H}) \times \mathbf{H}, \\ &\nabla \cdot \mathbf{v} = 0, \\ &\nabla \times \mathbf{H} = \sigma_e (\mathbf{E} + \mu_e \mathbf{v} \times \mathbf{H}), \\ &\nabla \times \mathbf{E} = \mathbf{0}, \quad \nabla \cdot \mathbf{E} = 0, \quad \nabla \cdot \mathbf{H} = 0, \quad \text{in} \quad \mathcal{S}, \end{aligned} \tag{2}$$

where $\mathbf{v}$ is the velocity field, p is the pressure, $\mathbf{E}$ and $\mathbf{H}$ are the electric and magnetic fields, respectively, ρ is the mass density (constant >0), μ_e is the magnetic permeability, σ_e is the electrical conductivity (μ_e, σ_e = constants > 0). We assume the region

$$\mathcal{S}^- = \{\mathbf{x} \in \mathbb{R}^3 : (x_1, x_3) \in \mathbb{R}^2, x_2 < 0\}$$

to be a vacuum (free space), and μ_e equal to the magnetic permeability of free space.

To Eq. (2) we append the usual boundary condition for $\mathbf{v}$:

$$v_2 = 0 \quad \text{at} \quad x_2 = 0. \tag{3}$$

Further, suppose that the tangential components of $\mathbf{H}$ and $\mathbf{E}$ are continuous through the plane $x_2 = 0$.

We are interested in the oblique plane stagnation-point flow, so that

$$v_1 = ax_1 + bx_2, \quad v_2 = -ax_2, \quad v_3 = 0, \quad x_1 \in \mathbb{R}, \quad x_2 \in \mathbb{R}^+, \tag{4}$$

with a, b constants ($a > 0$).

As known, the streamlines of such a flow are hyperbolas whose asymptotes have the equations:

$$x_2 = 0 \quad \text{and} \quad x_2 = -\frac{2a}{b}x_1.$$

These two straight-lines are degenerate streamlines too.

We summarize our results [14] concerning the influence upon such a flow of a uniform external electromagnetic field $(\mathbf{E}_0, \mathbf{H}_0)$. To this end, we consider three cases which, from a physical point of view, are significant.

2.1. CASE I

$$\mathbf{E}_0 = E_0\mathbf{e}_3, \quad \mathbf{H}_0 = \mathbf{0}.$$

Let the induced electromagnetic field $(\mathbf{E}^i, \mathbf{H}^i \equiv \mathbf{H})$ be in the form

$$\mathbf{E}^i = E_1^i\mathbf{e}_1 + E_2^i\mathbf{e}_2 + E_3^i\mathbf{e}_3,$$
$$\mathbf{H} = h(x_2)\mathbf{e}_1,$$

where $(\mathbf{e}_1, \mathbf{e}_2, \mathbf{e}_3)$ is the canonical base in $\mathbb{R}^3$. We provide the flow description in Fig. 1.

The boundary conditions require that

$$E_1^i = 0, \quad E_3^i = 0 \quad \text{at} \quad x_2 = 0,$$
$$h(0) = 0. \tag{5}$$

From $(2)_4$, $(2)_3$ follows that

$$h(x_2) = -\sigma_e E_0 e^{-\frac{ax_2^2}{2\eta_e}} \int_0^{x_2} e^{\frac{at^2}{2\eta_e}} dt, \quad x_2 \in \mathbb{R}^+, \tag{6}$$

with $\eta_e = \dfrac{1}{\sigma_e \mu_e}$ = electrical resistivity.

As far as the pressure field is concerned, from $(2)_1$ we get

$$p = -\frac{1}{2}\rho a^2\left(x_1^2 + x_2^2\right) - \frac{\mu_e}{2}h^2(x_2) + p_0, \quad x_1 \in \mathbb{R}, \quad x_2 \in \mathbb{R}^+,$$

where h is given by (6) and p_0 is the pressure in the stagnation point.

2.2. CASE II

$$\mathbf{E}_0 = \mathbf{0}, \quad \mathbf{H}_0 = H_0\mathbf{e}_1.$$

Let the induced electromagnetic field $(\mathbf{E}^i \equiv \mathbf{E}, \mathbf{H}^i)$ be in the form

$$\mathbf{E} = E_1\mathbf{e}_1 + E_2\mathbf{e}_2 + E_3\mathbf{e}_3,$$
$$\mathbf{H} = [h(x_2) + H_0]\mathbf{e}_1.$$

We provide the flow description in Fig. 2. We append the boundary conditions (5).

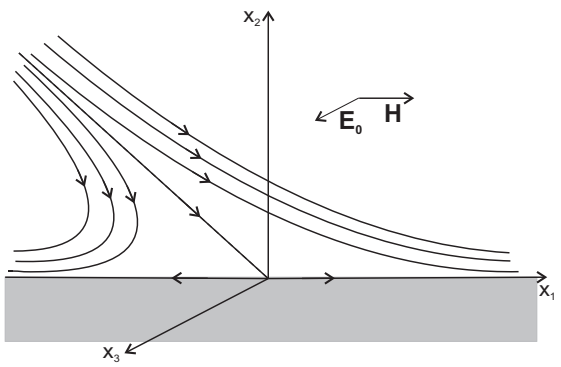

Fig. 1. Flow description in CASE I.

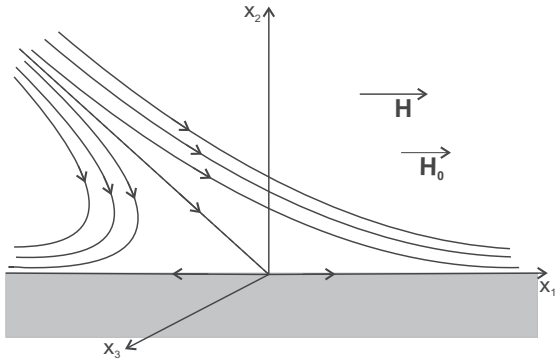

Fig. 2. Flow description in CASE II.

In this case we proved in [14] that

$$\mathbf{E} = \mathbf{0},$$
$$\mathbf{H} = H_0 e^{-\frac{ax_2^2}{2\eta_e}}\mathbf{e}_1,$$
$$p(x_1, x_2) = -\frac{1}{2}\rho a^2\left(x_1^2 + x_2^2\right) - \frac{\mu_e}{2}H_0^2 e^{-\frac{ax_2^2}{\eta_e}} + p_0, \quad x_1 \in \mathbb{R}, \quad x_2 \in \mathbb{R}^+.$$

2.3. CASE III

$$\mathbf{E}_0 = \mathbf{0}, \quad \mathbf{H}_0 = H_0(\cos\vartheta\mathbf{e}_1 + \sin\vartheta\mathbf{e}_2),$$

with ϑ fixed in $(0, \pi)$. We provide the flow description in Fig. 3.

Under the hypothesis that the magnetic Reynolds number is small, we neglect the induced magnetic field, as it is customary in the literature. We proved that $\mathbf{E} = \mathbf{0}$. Then

$$(\nabla \times \mathbf{H}) \times \mathbf{H} \simeq \sigma_e\mu_e(\mathbf{v} \times \mathbf{H}_0) \times \mathbf{H}_0 = \sigma_e\mu_e H_0^2[a\sin\vartheta x_1 + (b\sin\vartheta + a\cos\vartheta)x_2][-\sin\vartheta\mathbf{e}_1 + \cos\vartheta\mathbf{e}_2].$$

On substituting this approximation in $(2)_1$ we get:

$$\begin{aligned}
\frac{\partial p}{\partial x_1} &= -\rho a^2 x_1 - B_0^2\sigma_e\sin\vartheta[a\sin\vartheta x_1 + (b\sin\vartheta + a\cos\vartheta)x_2],\\
\frac{\partial p}{\partial x_2} &= -\rho a^2 x_2 + B_0^2\sigma_e\cos\vartheta[a\sin\vartheta x_1 + (b\sin\vartheta + a\cos\vartheta)x_2],\\
\frac{\partial p}{\partial x_3} &= 0 \Rightarrow p = p(x_1, x_2),
\end{aligned} \tag{7}$$

with $B_0 = \mu_e H_0$.

It is possible to find a function $p = p(x_1, x_2)$ satisfying Eq. (7) if and only if

$$\frac{\partial^2 p}{\partial x_1 \partial x_2} = \frac{\partial^2 p}{\partial x_2 \partial x_1}. \tag{8}$$

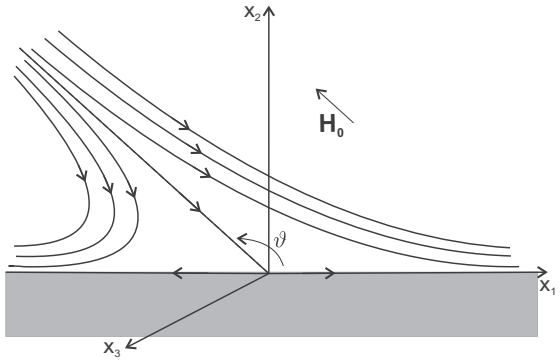

Fig. 3. Flow description in CASE III.

Taking into account (7), the previous condition furnishes

$$\sin\vartheta(2a\cos\vartheta + b\sin\vartheta) = 0. \tag{9}$$

From (9), we get

$$\tan\vartheta = -\frac{2a}{b}. \tag{10}$$

So the MHD oblique stagnation-point flow is possible if and only if $\mathbf{H}_0$ is parallel to the dividing streamline $x_2 = -\frac{2a}{b}x_1$.

We underline that in particular if $\mathbf{H}_0$ is normal to the plane $x_2 = 0$ (i.e. $\vartheta = \pi/2$), then there is no pressure that satisfies Eq. (16) and therefore the oblique stagnation-point flow given by (2) does not exist.

Under the condition (10), the pressure field has the form

$$p = -\frac{1}{2}\rho a^2(x_1^2 + x_2^2) - \frac{\sigma_e B_0^2}{4a^2 + b^2}\frac{a}{2}(2ax_1 + bx_2)^2 + p_0, \quad x_1 \in \mathbb{R}, \quad x_2 \in \mathbb{R}^+. \tag{11}$$

Our results can be summarized in the following:

Theorem 1. *Let a homogeneous, incompressible, electrically conducting inviscid fluid occupy the region $\mathcal{S}$. If we impress an external magnetic field $\mathbf{H}_0 = H_0(\cos\vartheta\mathbf{e}_1 + \sin\vartheta\mathbf{e}_2)$, $0 < \vartheta < \pi$, and we neglect the induced magnetic field, then the steady MHD oblique plane stagnation-point flow of such a fluid is possible if, and only if,*

$$\tan\vartheta = -\frac{2a}{b}, \quad \text{i.e.} \quad \mathbf{H}_0 = \frac{H_0}{\sqrt{4a^2 + b^2}}(-b\mathbf{e}_1 + 2a\mathbf{e}_2).$$

Moreover:

$$\mathbf{v} = (ax_1 + bx_2)\mathbf{e}_1 - ax_2\mathbf{e}_2,$$
$$p = -\frac{1}{2}\rho a^2(x_1^2 + x_2^2) - \frac{\sigma_e B_0^2}{4a^2 + b^2}\frac{a}{2}(2ax_1 + bx_2)^2 + p_0, \quad x_1 \in \mathbb{R}, \quad x_2 \in \mathbb{R}^+.$$

Remark 2. In order to study oblique stagnation-point flow for micropolar fluids, it is convenient to consider a more general flow. More precisely, we suppose the fluid obliquely impinging on the flat plane $x_2 = A$ and

$$v_1 = ax_1 + b(x_2 - B), \quad v_2 = -a(x_2 - A), \quad v_3 = 0, \quad x_1 \in \mathbb{R}, \quad x_2 \geqslant A, \tag{12}$$

with A, B = constants.

In this way, the stagnation point is $(\frac{b}{a}(B - A), A)$.

In this case, the streamlines are the hyperbolas whose asymptotes are $x_2 = -\frac{2a}{b}x_1 + 2B - A$ and $x_2 = A$.

As it is easy to verify, in the absence of $(\mathbf{E}, \mathbf{H})$, the pressure field is given by:

$$p = -\frac{1}{2}\rho a^2\left\{\left[x_1 - \frac{b}{a}(B - A)\right]^2 + (x_2 - A)^2\right\} + p_0.$$

We underline that under these new assumptions, all previous results continue to hold by replacing x_1, x_2 with $x_1 - \frac{b}{a}(B - A), x_2 - A$, respectively.

3. Micropolar fluids

Consider the steady two-dimensional oblique stagnation-point flow of an electrically conducting homogeneous incompressible micropolar fluid towards a flat surface coinciding with the plane $x_2 = 0$, the flow being confined to the region $\mathcal{S}$. In the absence of external mechanical body forces and body couples, the MHD equations for such a fluid are [3]

$$\begin{aligned}
&\mathbf{v}\cdot\nabla\mathbf{v} = -\frac{1}{\rho}\nabla p + (\nu + \nu_r)\triangle\mathbf{v} + 2\nu_r(\nabla\times\mathbf{w}) + \frac{\mu_e}{\rho}(\nabla\times\mathbf{H})\times\mathbf{H},\\
&\nabla\cdot\mathbf{v} = 0,\\
&I\mathbf{v}\cdot\nabla\mathbf{w} = \lambda\triangle\mathbf{w} + \lambda_0\nabla(\nabla\cdot\mathbf{w}) - 4\nu_r\mathbf{w} + 2\nu_r(\nabla\times\mathbf{v}),
\end{aligned} \tag{13}$$

together with $(2)_3$–$(2)_6$, where $\mathbf{w}$ is the microrotation field, ν is the kinematic newtonian viscosity coefficient, ν_r is the microrotation viscosity coefficient, λ, λ_0 (positive constants) are material parameters related to the coefficient of angular viscosity and I is the microinertia coefficient.

We notice that in [1,2], Eq. (13) are slightly different, as they are deduced as a special case of much more general model of microfluids. For the details, we refer to [3], p. 23.

As far as the boundary conditions are concerned, of course, we modify condition (3) and prescribe the appropriate boundary condition for the microrotation **w**, i.e.

$$\mathbf{v}|_{x_2=0} = \mathbf{0}, \mathbf{w}|_{x_2=0} = \mathbf{0} \quad \text{(strict adherence condition)}. \tag{14}$$

Other boundary conditions are possible. We refer to Eringen ([1], p. 17–18) for a complete discussion. In our studies we will always assume the strict adherence condition.

We search **v**, **w** in the following form

$$\begin{aligned} &v_1 = ax_1 f'(x_2) + bg(x_2), v_2 = -af(x_2), \quad v_3 = 0, \\ &w_1 = 0, \quad w_2 = 0, \quad w_3 = x_1 F(x_2) + G(x_2), \quad x_1 \in \mathbb{R}, \quad x_2 \in \mathbb{R}^+, \end{aligned} \tag{15}$$

where f, g, F, G are unknown functions.

The conditions (14) supply

$$\begin{aligned} &f(0) = 0, \quad f'(0) = 0, \quad g(0) = 0, \\ &F(0) = 0, \quad G(0) = 0. \end{aligned} \tag{16}$$

Moreover, as is customary when studying oblique plane stagnation-point flow for viscous fluids, we assume that at infinity, the flow approaches the flow of an inviscid fluid given by (12) [6,17,15].

Therefore, to (15) we must append also the following conditions

$$\begin{aligned} &\lim_{x_2\to+\infty} f'(x_2) = 1, \quad \lim_{x_2\to+\infty} g'(x_2) = 1, \\ &\lim_{x_2\to+\infty} F(x_2) = 0, \quad \lim_{x_2\to+\infty} G(x_2) = -\frac{b}{2}. \end{aligned} \tag{17}$$

Conditions $(17)_{3,4}$ mean that at infinity, $\mathbf{w} = \frac{1}{2}\nabla \times \mathbf{v}$, i.e. the micropolar fluid behaves like a classical fluid.

In all the following cases, when we will refer to inviscid fluid, all results have to be modified by replacing x_1, x_2 with $x_1 - \frac{b}{a}(B - A), x_2 - A$, respectively. In particular, the asymptotic behaviour of f and g at infinity is related to the constants A, B, in the following way:

$$\lim_{x_2\to+\infty} [f(x_2) - x_2] = -A, \lim_{x_2\to+\infty} [g(x_2) - x_2] = -B. \tag{18}$$

As we will see, A is determined as part of the solution of the orthogonal flow, while B is a free parameter.

In order to study the influence of a uniform external electromagnetic field, we consider the three cases analysed in the previous section.

3.1. CASE I-M

By proceeding as for an inviscid fluid, from $(2)_3$, $(2)_4$ and boundary conditions for electromagnetic field, we obtain $\mathbf{E} = E_0\mathbf{e}_3$ and the induced magnetic field $h(x_2)$ satisfies

$$h' + \frac{a}{\eta_e} fh = -\eta_e E_0, \quad x_2 > 0, \quad h(0) = 0. \tag{19}$$

If we regard f as a known function, we arrive at

$$h(x_2) = -\sigma_e E_0 e^{-\frac{a}{\eta_e}\int_0^{x_2} f(t)dt} \int_0^{x_2} e^{\frac{a}{\eta_e}\int_0^{s} f(t)dt} ds, \quad x_2 \in \mathbb{R}^+. \tag{20}$$

As is easy to verify, the induced magnetic fields given by (20) and (6) have the same asymptotic behaviour at infinity $\left(\sim -\frac{\eta_e E_0 \sigma_e}{a(x_2 - A)}\right)$.

In order to determine p, f, g, F, G we substitute (15) in $(13)_{1,3}$. After some calculations, we arrive at

$$\begin{aligned} &p = p(x_1, x_2), \\ &ax_1\left[(\nu + \nu_r)f''' + aff'' - af'^2 + \frac{2\nu_r}{a}F'\right] + b\left[(\nu + \nu_r)g'' + a(fg' - f'g) + \frac{2\nu_r}{b}G'\right] = \frac{1}{\rho}\frac{\partial p}{\partial x_1}, \\ &(\nu + \nu_r)af'' + a^2 f'f + 2\nu_r F + \frac{\mu_e}{\rho}h'h = -\frac{1}{\rho}\frac{\partial p}{\partial x_2}, \\ &x_1\left[\alpha F'' + Ia(F'f - Ff') - 2\nu_r(2F + af'')\right] + \lambda G'' + I(aG'f - bFg) - 2\nu_r(2G + bg') = 0. \end{aligned} \tag{21}$$

Then, by integrating $(21)_3$, we find

$$p(x_1, x_2) = -\frac{1}{2}\rho a^2 f^2(x_2) - \rho a(\nu + \nu_r)f'(x_2) - 2\nu_r\rho\int_0^{x_2} F(s)ds - \frac{\mu_e}{2}h^2(x_2) + P(x_1),$$

where the function $P(x_1)$ is determined supposing that, far from the wall, the pressure p has the same behaviour as for an inviscid electroconducting fluid, whose velocity is given by (12).

Therefore, since the induced electromagnetic fields given by (20) and (6) have the same asymptotic behaviour, under the assumption $F \in L^1([0,+\infty))$, by virtue of (17) and (18), we get

$$P(x_1) = -\rho\frac{a^2}{2}\left[x_1 - \frac{b}{a}(B-A)\right]^2 + p_0 + \rho a(v+v_r).$$

Finally, the pressure field assumes the form

$$p(x_1,x_2) = -\rho\frac{a^2}{2}\left[x_1^2 - 2\frac{b}{a}(B-A)x_1 + f^2(x_2)\right] - \rho a(v+v_r)f'(x_2) - 2v_r\rho\int_0^{x_2} F(s)ds - \frac{\mu_e}{2}h^2(x_2) + p_0^*, \tag{22}$$

with $p_0^* = p_0 + \rho a(v+v_r) - \rho\frac{b^2}{2}(B-A)^2$.

In consideration of (22), we obtain the ordinary differential system

$$\begin{aligned}
&\frac{v+v_r}{a}f''' + ff'' - f'^2 + 1 + \frac{2v_r}{a^2}F' = 0,\\
&\frac{v+v_r}{a}g'' + fg' - gf' + \frac{2v_r}{ab}G' = B - A,\\
&\lambda F'' + aI(fF' - f'F) - 2v_r(2F + af'') = 0,\\
&\lambda G'' + I(afG' - bgF) - 2v_r(2G + bg') = 0.
\end{aligned} \tag{23}$$

To these equations we append the boundary conditions (16) and (17).

We remark that the system (23) governs the oblique stagnation-point flow of an inert electromagnetic micropolar fluid, as is easy to verify. In literature, such a flow has been studied in [9,10] under restrictive assumptions upon the material parameters, and following a different approach.

Remark 3. If $v_r = 0$, then $(23)_1$ and $(23)_2$ are the equations governing the oblique stagnation-point flow of a Newtonian fluid.

We observe that $(23)_1$ and $(23)_3$ have the same form as the equations found by Guram and Smith [7] for the orthogonal stagnation-point flow of a micropolar fluid.

Theorem 4. *Let a homogeneous, incompressible, electrically conducting micropolar fluid occupy the region $\mathcal{S}$. The steady MHD oblique plane stagnation-point flow of such a fluid has the following form when an external uniform electric field $\mathbf{E}_0 = E_0\mathbf{e}_3$ is impressed:*

$$\begin{aligned}
&\mathbf{v} = [ax_1f'(x_2) + bg(x_2)]\mathbf{e}_1 - af(x_2)\mathbf{e}_2, \quad \mathbf{H} = h(x_2)\mathbf{e}_1, \quad \mathbf{E} = E_0\mathbf{e}_3,\\
&\mathbf{w} = [x_1F(x_2) + G(x_2)]\mathbf{e}_3,\\
&p = -\rho\frac{a^2}{2}\left[x_1^2 - 2\frac{b}{a}(B-A)x_1 + f^2(x_2)\right] - \rho a(v+v_r)f'(x_2) - 2v_r\rho\int_0^{x_2} F(s)ds - \frac{\mu_e}{2}h^2(x_2) + p_0^*,\\
&x_1 \in \mathbb{R}, \quad x_2 \in \mathbb{R}^+,
\end{aligned}$$

where (f,g,F,G) satisfies the problem (23), (16), and (17), provided $F \in L^1([0,+\infty))$, and $h(x_2)$ is given by (20).

Now we write the system (23), together with the conditions (16) and (17), in dimensionless form. To this end we put

$$\begin{aligned}
&\eta = \sqrt{\frac{a}{v+v_r}}x_2, \phi(\eta) = \sqrt{\frac{a}{v+v_r}}f\left(\sqrt{\frac{v+v_r}{a}}\eta\right),\\
&\gamma(\eta) = \sqrt{\frac{a}{v+v_r}}g\left(\sqrt{\frac{v+v_r}{a}}\eta\right), \quad \Phi(\eta) = \frac{2v_r}{a^2}\sqrt{\frac{a}{v+v_r}}F\left(\sqrt{\frac{v+v_r}{a}}\eta\right),\\
&\Gamma(\eta) = \frac{2v_r}{b(v+v_r)}G\left(\sqrt{\frac{v+v_r}{a}}\eta\right), \quad \Psi(\eta) = \frac{1}{\sigma_eE_0}\sqrt{\frac{a}{v+v_r}}h\left(\sqrt{\frac{v+v_r}{a}}\eta\right).
\end{aligned}$$

So system (23) and Eq. (19) can be written as

$$\begin{aligned}
&\phi''' + \phi\phi'' - \phi'^2 + 1 + \Phi' = 0,\\
&\gamma'' + \phi\gamma' - \phi'\gamma + \Gamma' = \beta - \alpha,\\
&\Phi'' + c_3(\phi\Phi' - \phi'\Phi) - c_2\Phi - c_1\phi'' = 0,\\
&\Gamma'' + c_3(\phi\Gamma' - \Phi\gamma) - c_2\Gamma - c_1\gamma' = 0,\\
&\Psi' + R_m\phi\Psi = -1,
\end{aligned} \tag{24}$$

where

$$c_1 = \frac{4v_r^2}{\lambda a}, \quad c_2 = \frac{4v_r(v+v_r)}{\lambda a}, \quad c_3 = \frac{I}{\lambda}(v+v_r),$$
$$\alpha = \sqrt{\frac{a}{v+v_r}}A, \quad \beta = \sqrt{\frac{a}{v+v_r}}B, \quad R_m = \frac{v+v_r}{\eta_e} = \text{magnetic Reynolds number}.$$

The boundary conditions in dimensionless form become:

$$\begin{aligned} &\phi(0) = 0, \quad \phi'(0) = 0, \quad \gamma(0) = 0, \\ &\Phi(0) = 0, \quad \Gamma(0) = 0, \\ &\Psi(0) = 0, \\ &\lim_{\eta\to+\infty} \phi'(\eta) = 1, \quad \lim_{\eta\to+\infty} \gamma'(\eta) = 1 \\ &\lim_{\eta\to+\infty} \Phi(\eta) = 0, \quad \lim_{\eta\to+\infty} \Gamma(\eta) = -\frac{c_1}{c_2}. \end{aligned} \tag{25}$$

The last equation in (24), if we regard ϕ as a known function, can be formally integrated to give

$$\Psi(\eta) = -e^{-R_m\int_0^\eta \phi(s)ds}\int_0^\eta e^{R_m\int_0^t \phi(s)ds}dt, \quad \eta \in \mathbb{R}^+.$$

The remaining equations have to be integrated numerically.

Remark 5. Along the wall $x_2 = 0$, there are three important coordinates: the origin $x_1 = 0$ which is the stagnation-point for the flow, the point $x_1 = x_p$ of maximum pressure, and the point $x_1 = x_s$ of zero tangential stress (zero skin friction) where the dividing streamline of equation

$$\xi\phi(\eta) + \frac{b}{a}\int_0^\eta \gamma(s)ds = 0, \quad \xi = \sqrt{\frac{v+v_r}{a}}x_1 \tag{26}$$

meets the boundary.

In consideration of (22), we see that

$$x_p = b\sqrt{\frac{v+v_r}{a^3}}(\beta-\alpha) \tag{27}$$

and so x_p does not depend on h.

The wall shear stress is given by

$$\tau = \rho(v+v_r)\frac{\partial v_1}{\partial x_2}|_{x_2=0};$$

the position x_s is obtained by putting $\tau = 0$. Hence

$$x_s = -b\sqrt{\frac{v+v_r}{a^3}}\frac{\gamma'(0)}{\phi''(0)}. \tag{28}$$

We note that the ratio $\frac{x_p}{x_s} = (\alpha-\beta)\frac{\phi''(0)}{\gamma'(0)}$ is the same for all angles of incidence.

Finally, we recall that studying the small-η behaviour of $\frac{\int_0^\eta \gamma(s)ds}{\phi(\eta)}$, the slope of the dividing streamline at the wall is given by:

$$m_s = -\frac{3a[\phi''(0)]^2}{b\{[\beta-\alpha-\Gamma'(0)]\phi''(0) + [1+\Phi'(0)]\gamma'(0)\}}$$

and does not depend on the kinematic viscosities. Thus, the ratio of this slope to that of the dividing streamline at infinity $\left(m_i = -\frac{2a}{b}\right)$ is the same for all oblique stagnation-point flows and is given by

$$\frac{m_s}{m_i} = \frac{3}{2}\frac{[\phi''(0)]^2}{[\beta-\alpha-\Gamma'(0)]\phi''(0) + [1+\Phi'(0)]\gamma'(0)}. \tag{29}$$

This ratio is independent of a and b, depending only upon the constant pressure gradient parallel to the boundary through $B-A$, as with Newtonian fluids [19].

3.2. CASE II-M

By proceeding as one would with an inviscid fluid, from $(2)_3$ and $(2)_4$ and boundary conditions for electromagnetic field, we get

$$h' + \frac{a}{\eta_e} f h = -\frac{a}{\eta_e} f H_0, \quad x_2 > 0, \quad h(0) = 0. \tag{30}$$

The integration of (30) leads to

$$h(x_2) = H_0 \left(e^{-\frac{a}{\eta_e}\int_0^{x_2} f(t)dt} - 1 \right), \quad x_2 \in \mathbb{R}^+, \tag{31}$$

so that

$$\mathbf{H} = H_0 e^{-\frac{a}{\eta_e}\int_0^{x_2} f(s)ds} \mathbf{e}_1.$$

The pressure field, as is easy to verify, becomes

$$p(x_1, x_2) = -\rho \frac{a^2}{2} \left[x_1^2 - 2\frac{b}{a}(B - A)x_1 + f^2(x_2) \right] - \rho a(\nu + \nu_r) f'(x_2) - 2\nu_r \rho \int_0^{x_2} F(s)ds - \frac{\mu_e}{2}[h(x_2) + H_0]^2 + p_0^*, \tag{32}$$

where (f, g, F, G) satisfies system (23), together with boundary conditions (16) and (17).

Therefore, in this case as well, the uniform external electromagnetic field does not influence the flow.

Thus, we obtain the following:

Theorem 6. *Let a homogeneous, incompressible, electrically conducting micropolar fluid occupy the region $\mathcal{S}$. The steady MHD oblique plane stagnation-point flow of such a fluid has the following form when a uniform external magnetic field $\mathbf{H}_0 = H_0\mathbf{e}_1$ is impressed:*

$$\mathbf{v} = [a x_1 f'(x_2) + b g(x_2)]\mathbf{e}_1 - a f(x_2)\mathbf{e}_2, \quad \mathbf{H} = [H_0 + h(x_2)]\mathbf{e}_1, \quad \mathbf{E} = E_0\mathbf{e}_3,$$
$$\mathbf{w} = [x_1 F(x_2) + G(x_2)]\mathbf{e}_3,$$
$$p = -\rho \frac{a^2}{2} \left[x_1^2 - 2\frac{b}{a}(B - A)x_1 + f^2(x_2) \right] - \rho a(\nu + \nu_r) f'(x_2) - 2\nu_r \rho \int_0^{x_2} F(s)ds - \frac{\mu_e}{2}[h(x_2) + H_0]^2 + p_0^*, \quad x_1 \in \mathbb{R}, \quad x_2 \in \mathbb{R}^+,$$

where (f, g, F, G) satisfies the problem (23), (16) and (17), provided $F \in L^1([0, +\infty))$, and $h(x_2)$ is given by (31).

In dimensionless form, $h(x_2)$ becomes

$$\Psi(\eta) = e^{-R_m \int_0^{\eta} \phi(t)dt} - 1, \quad \eta \in \mathbb{R}^+, \tag{33}$$

where

$$\Psi(\eta) = \frac{1}{H_0} h\left(\sqrt{\frac{\nu + \nu_r}{a}}\eta \right).$$

Of course, Remark 3 continues to hold in this case.

3.3. CASE III-M

Taking into account the results obtained for an inviscid fluid, we assume

$$\mathbf{H}_0 = \frac{H_0}{\sqrt{4a^2 + b^2}}(-b\mathbf{e}_1 + 2a\mathbf{e}_2), \mathbf{E}_0 = \mathbf{0}.$$

As in CASE III, for inviscid fluid, we deduce

$$\mathbf{E} = \mathbf{0} \Rightarrow \nabla \times \mathbf{H} = \sigma_e \mu_e (\mathbf{v} \times \mathbf{H}).$$

Further, we neglect the induced magnetic field, replacing $(13)_1$ with

$$\mathbf{v} \cdot \nabla \mathbf{v} = -\frac{1}{\rho}\nabla p + (\nu + \nu_r)\triangle \mathbf{v} + 2\nu_r(\nabla \times \mathbf{w}) + \frac{\mu_e}{\rho}(\mathbf{v} \times \mathbf{H}_0) \times \mathbf{H}_0. \tag{34}$$

This approximation is motivated by physical arguments for MHD flow at small magnetic Reynolds numbers.

We substitute (15) into (34) to determine p, f, g, F, G. This yields

$$\begin{aligned}
&p = p(x_1, x_2),\\
&ax_1\left[(v+v_r)f''' + aff'' - af'^2 + \frac{2v_r}{a}F' - 4a^2\frac{\sigma_e}{\rho}\frac{B_0^2}{4a^2+b^2}f'\right]\\
&\quad + b\left[(v+v_r)g'' + a(fg' - f'g) + \frac{2v_r}{b}G' - 2a^2\frac{\sigma_e}{\rho}\frac{B_0^2}{4a^2+b^2}(2g-f)\right] = \frac{1}{\rho}\frac{\partial p}{\partial x_1},\\
&(v+v_r)af'' + a^2f'f + 2v_rF + \frac{\sigma_e}{\rho}\frac{B_0^2}{4a^2+b^2}\left[2a^2bx_1f' + ab^2(2g-f)\right] = -\frac{1}{\rho}\frac{\partial p}{\partial x_2}.
\end{aligned} \tag{35}$$

The integration of $(35)_3$ gives

$$p(x_1,x_2) = -\frac{1}{2}\rho a^2f^2(x_2) - \rho a(v+v_r)f'(x_2) - 2v_r\rho\int_0^{x_2}F(s)ds - \sigma_e\frac{B_0^2}{4a^2+b^2}\left\{2a^2bx_1f(x_2) + ab^2\int_0^{x_2}[2g(s)-f(s)]ds\right\} + P(x_1),$$

where $P(x_1)$ has to be found as in CASES I-M, II-M.

After some calculations, we obtain

$$P(x_1) = -\rho\frac{a^2}{2}\left(1 + \frac{4a}{\rho}\frac{\sigma_eB_0^2}{4a^2+b^2}\right)\left[x_1 - \frac{b}{a}(B-A)\right]^2 + p_0'$$

with p_0' constant.

So the pressure field is:

$$\begin{aligned}
p(x_1,x_2) = &-\rho\frac{a^2}{2}\left[x_1^2 - 2\frac{b}{a}(B-A)x_1 + f^2(x_2)\right] - \rho a(v+v_r)f'(x_2) - 2v_r\rho\int_0^{x_2}F(s)ds\\
&- \frac{\sigma_eB_0^2}{4a^2+b^2}\left\{2a^2bx_1f(x_2) + \int_0^{x_2}[2g(s)-f(s)]ds + 2a^3\left[x_1^2 - \frac{2b}{a}(B-A)x_1\right]\right\} + p_0^*, \quad x_1\in\mathbb{R}, \quad x_2\in\mathbb{R}^+.
\end{aligned} \tag{36}$$

The constant p_0^* represents the pressure at the stagnation point.

Table 1
CASE I-M: descriptive quantities of motion for some values of c_1, c_2, c_3.

c_1	c_2	c_3	α	$\beta-\alpha$	$\phi''(0)$	$\gamma'(0)$	$\Phi'(0)$	$\Gamma'(0)$	$\frac{x_p}{x_s}$	$\frac{m_s}{m_i}$	$\bar\eta_\phi$	$\bar\eta_\gamma$
0.1	1.5	0.1	0.6446	−0.6446	1.2218	1.3647	−0.0532	−0.0892	0.5771	3.6492	2.5556	3.0667
				0	1.2218	0.5771	−0.0532	−0.0550	0	3.6495	2.5556	3.1944
				0.6446	1.2218	−0.2105	−0.0532	−0.0207	3.7415	3.6498	2.5556	3.2370
		0.5	0.6448	−0.6448	1.2231	1.3651	−0.0510	−0.0889	0.5777	3.6455	2.5556	3.0667
				0	1.2231	0.5765	−0.0510	−0.0560	0	3.6455	2.5556	3.1944
				0.6448	1.2231	−0.2121	−0.0510	−0.0231	3.7177	3.6455	2.5556	3.2370
	3.0	0.1	0.6453	−0.6453	1.2250	1.3817	−0.0444	−0.0658	0.5721	3.6871	2.5556	3.0667
				0		0.5912	−0.0444	−0.0372	0	3.6872	2.5556	3.1944
				0.6453	1.2250	−0.1993	−0.0444	−0.0085	3.9656	3.6872	2.5556	3.2370
		0.5	0.6454	−0.6454	1.2256	1.3822	−0.0434	−0.0652	0.5723	3.6871	2.5556	3.0667
				0	1.2256	0.5912	−0.0434	−0.0372	0	3.6871	2.5556	3.1944
				0.6454	1.2256	−0.1998	−0.0434	−0.0092	3.9577	3.6871	2.5556	3.2370
0.5	1.5	0.1	0.6311	−0.6311	1.1780	1.1970	−0.2659	−0.4280	0.6211	3.2546	2.2148	2.5556
				0	1.1780	0.4534	−0.2659	−0.2602	0	3.2560	2.2148	2.7259
				0.6311	1.1780	−0.2903	−0.2659	−0.0923	2.5611	3.2574	2.2148	2.7259
		0.5	0.6321	−0.6321	1.1848	1.1987	−0.2553	−0.4275	0.6248	3.2381	2.2148	2.5556
				0	1.1848	0.4498	−0.2553	−0.2661	0	3.2383	2.2148	2.7259
				0.6321	1.1848	−0.2991	−0.2553	−0.1047	2.5034	3.2385	2.2148	2.8963
	3.0	0.1	0.6351	−0.6351	1.1943	1.2825	−0.2220	−0.3200	0.5914	3.4426	2.3852	2.9389
				0	1.1943	0.5240	−0.2220	−0.1790	0	3.4429	2.3852	3.0667
				0.6351	1.1943	−0.2345	−0.2220	−0.0380	3.2343	3.4433	2.3852	3.0667
		0.5	0.6356	−0.6356	1.1972	1.2846	−0.2173	−0.3174	0.5923	3.4426	2.3852	2.9389
				0	1.1972	0.5237	−0.2173	−0.1793	0	3.4426	2.3852	3.1596
				0.6356	1.1972	−0.2372	−0.2173	−0.0412	3.2074	3.4427	2.3852	3.0667

Then, $(35)_2$ supplies

$$\begin{aligned}&\frac{\nu+\nu_r}{a}f'''+ff''-f'^2+1+\frac{2\nu_r}{a^2}F'+M^2(1-f')=0,\\&\frac{\nu+\nu_r}{a}g''+fg'-gf'+\frac{2\nu_r}{ab}G'+M^2(f-g)=(1+M^2)(B-A),\end{aligned}\tag{37}$$

where

$$M=2B_0\sqrt{\frac{a\sigma_e}{\rho(4a^2+b^2)}}$$

is the Hartmann number.

Of course (f,g,F,G) also satisfies the equations $(23)_{3,4}$. We append boundary conditions (16) and (17) to the system in (37) and $(23)_{3,4}$.

We remark that, unlike the previous cases, the external electromagnetic field modifies the flow; if $M=0$, then the system (37) and $(23)_{3,4}$ reduces to the system (23).

Theorem 7. *Let a homogeneous, incompressible, electrically conducting micropolar fluid occupy the region $\mathcal{S}$. If we impress the external magnetic field*

$$\mathbf{H}_0=\frac{H_0}{\sqrt{4a^2+b^2}}(-b\mathbf{e}_1+2a\mathbf{e}_2)$$

and if we neglect the induced magnetic field, then the steady MHD oblique plane stagnation-point flow of such a fluid has the form

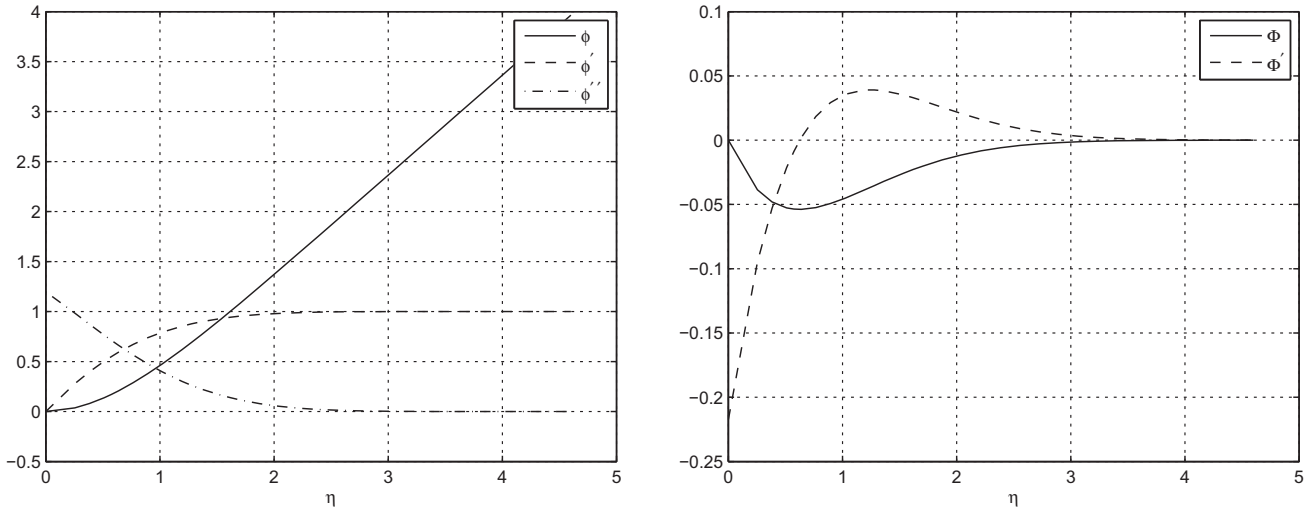

Fig. 4. CASE I-M: plots showing the behaviour of ϕ, ϕ', ϕ'' and Φ, Φ', respectively for $c_1=0.5$, $c_2=3.0$, $c_3=0.5$.

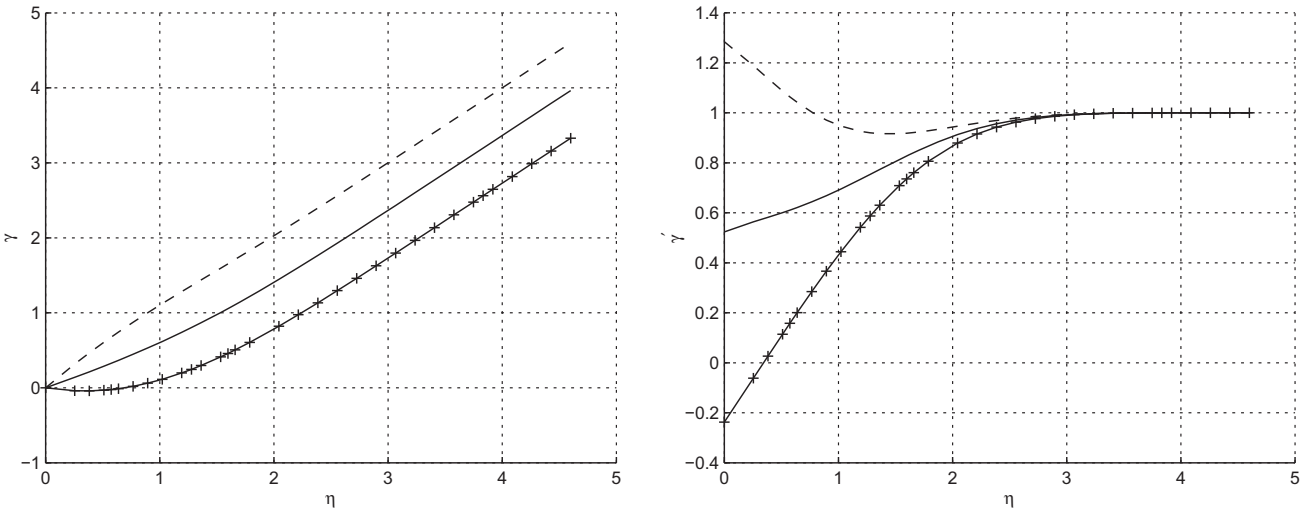

Fig. 5. CASE I-M: Figs. 5_1 and 5_2 show γ and γ' for $c_1=0.5$, $c_2=3.0$, $c_3=0.5$ and with, from above, $\beta-\alpha=-\alpha$, 0, α, respectively.

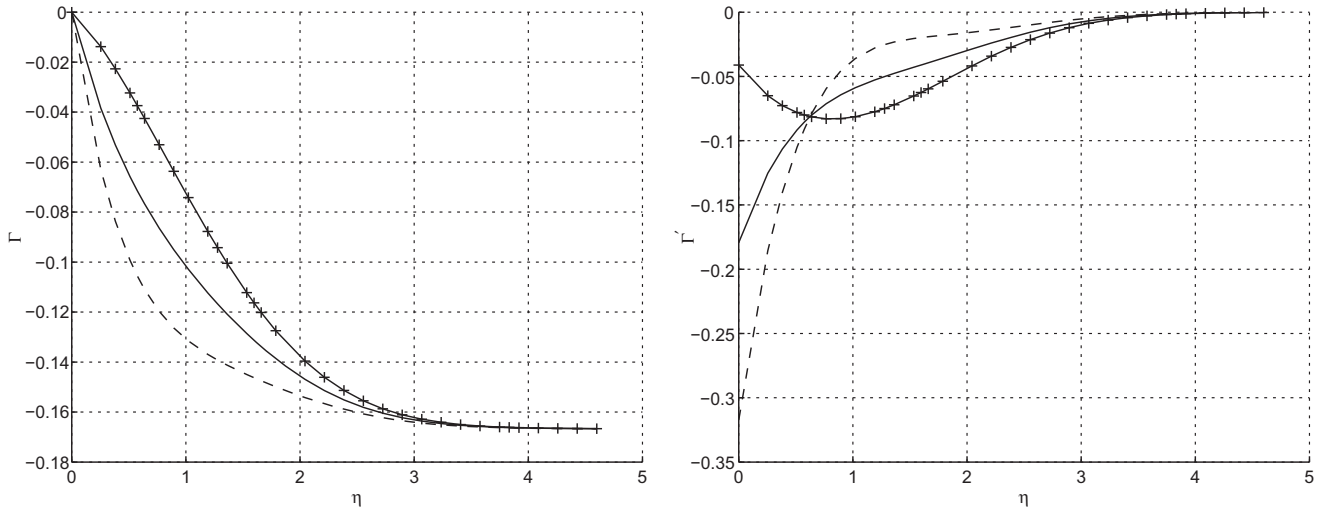

Fig. 6. CASE I-M: Figs. 6_1 and 6_2 show Γ and Γ' for $c_1 = 0.5$, $c_2 = 3.0$, $c_3 = 0.5$ and with, from above, $\beta - \alpha = -\alpha$, 0, α, respectively.

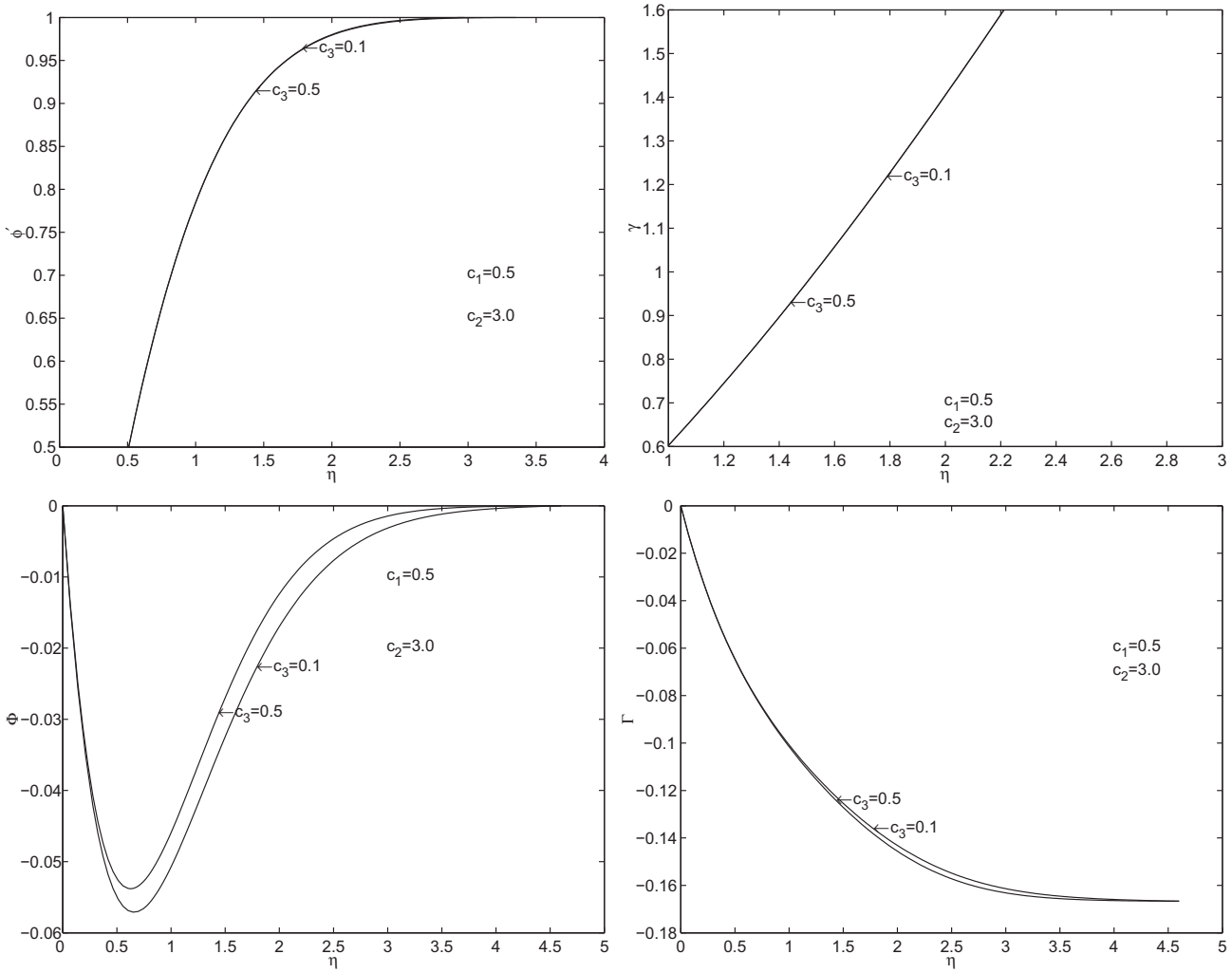

Fig. 7. CASE I-M: plots showing the behaviour of ϕ', γ, Φ and Γ for $c_1 = 0.5$, $c_2 = 3.0$ fixed, and for different values of c_3.

$$\mathbf{v} = [ax_1 f'(x_2) + bg(x_2)]\mathbf{e}_1 - af(x_2)\mathbf{e}_2,$$
$$\mathbf{w} = [x_1 F(x_2) + G(x_2)]\mathbf{e}_3, \mathbf{E} = \mathbf{0},$$
$$p = -\rho\frac{a^2}{2}\left[x_1^2 - 2\frac{b}{a}(B-A)x_1 + f^2(x_2)\right] - \rho a(v+v_r)f'(x_2) - 2v_r\rho\int_0^{x_2} F(s)ds$$
$$-\frac{\sigma_e B_0^2}{4a^2+b^2}\left\{2a^2 b x_1 f(x_2) + \int_0^{x_2}[2g(s) - f(s)]ds + 2a^3\left[x_1^2 - \frac{2b}{a}(B-A)x_1\right]\right\} + p_0^*, \quad x_1 \in \mathbb{R}, \quad x_2 \in \mathbb{R}^+,$$

where (f,g,F,G) satisfies problem (37), (23)$_{3,4}$, (16), and (17), provided $F \in L^1([0,+\infty))$.

In dimensionless form, we arrive at the following ordinary differential problem:

$$\begin{aligned}
&\phi''' + \phi\phi'' - \phi'^2 + 1 + \Phi' + M^2(1-\phi') = 0,\\
&\gamma'' + \phi\gamma' - \phi'\gamma + \Gamma' + M^2(\phi-\gamma) = (1+M^2)(\beta-\alpha),\\
&\Phi'' + c_3(\phi\Phi' - \phi'\Phi) - c_2\Phi - c_1\phi'' = 0,\\
&\Gamma'' + c_3(\phi\Gamma' - \Phi\gamma) - c_2\Gamma - c_1\gamma' = 0.
\end{aligned} \tag{38}$$

To system (38), we append boundary conditions (25).

Problem (38) and (25) will be solved numerically in Section 4 for some values of c_1, c_2, c_3, M.

Remark 8. The points $x_1 = x_p$ of maximum pressure and $x_1 = x_s$ of zero tangential stress on $x_2 = 0$ are formally the same as in CASE I-M and II-M. However, these points depend on M.

Finally the slope of the dividing streamline at the wall is given by:

$$m_s = -\frac{3a[\phi''(0)]^2}{b\{[(\beta-\alpha)(1+M^2) - \Gamma'(0)]\phi''(0) + [1+M^2+\Phi'(0)]\gamma'(0)\}}.$$

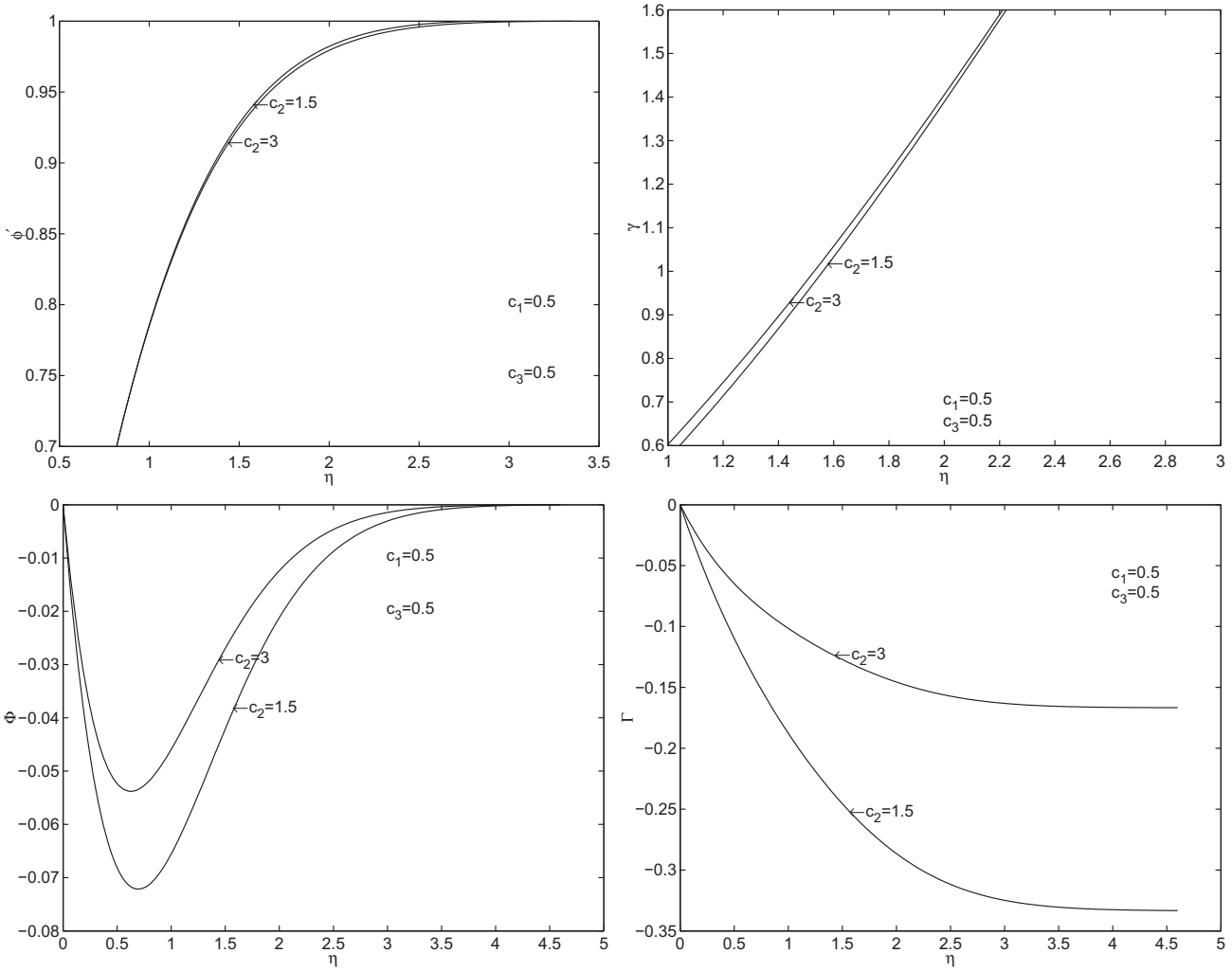

Fig. 8. CASE I-M: plots showing the behaviour of ϕ', γ, Φ and Γ for $c_1 = 0.5$, $c_3 = 0.5$ fixed, and for different values of c_2.

4. Numerical results and discussion

In this section we discuss the numerical solutions of the problems studied in CASES I, II, III-M. These numerical solutions are obtained using the MATLAB routine **bvp4c**. This routine is a finite difference code that implements the three-stage Lobatto IIIa formula. This is a collocation formula and here the collocation polynomial provides a C^1-continuous solution that is fourth-order accurate uniformly in [0,4.6]. Mesh selection and error control are based on the residual of the continuous solution. Here the maximum residual is 10^{-4}, while the relative and absolute tolerance are 10^{-3} and 10^{-6} respectively. This method was used and described in [18].

4.1. CASE I-M

We have solved problem (24) and (25) numerically.

The values of the parameters c_1, c_2, c_3 were chosen according to Guram and Smith [7] and are given in Table 1, where we also assign some values to β (i.e. $\beta - \alpha = -\alpha, 0, \alpha$). The consequent values of $\alpha, \phi''(0), \gamma'(0), \Phi'(0), \Gamma'(0), \frac{x_p}{x_s}, \frac{m_s}{m_i}, \bar{\eta}_\phi, \bar{\eta}_\gamma$ are reported in this table. We denote by $\bar{\eta}_\phi$ the value of η at which $\phi' = 0.99$ (so when $\eta > \bar{\eta}_\phi$, then $\phi = \eta - \alpha$), while $\bar{\eta}_\gamma$ is the value of η at which $\gamma' = 0.99$ (if $\beta - \alpha \geqslant 0$) or $\gamma' = 1.01$ (if $\beta - \alpha < 0$). So when $\eta > \bar{\eta}_\gamma$ then $\gamma = \eta - \beta$.

We see that $\bar{\eta}_\gamma$ is always greater than $\bar{\eta}_\phi$, as in the Newtonian case [14]. Hence the influence of the viscosity on the velocity appears only in a layer of thickness $\bar{\eta}_\gamma$ lining the boundary. We remark that the thickness of the layer affected by the viscosity is proportional to $\sqrt{\frac{\nu + \nu_r}{a}}$ and it is larger than that in the orthogonal stagnation-point flow.

From Table 1 it appears that if we fix two parameters among c_1,c_2, c_3, then the values of α, $\phi''(0)$, $\gamma'(0)$, $\Phi'(0)$, $\Gamma'(0)$ have the following behaviour:

they increase as c_2 increases,
they lower as c_1 or c_3 increases.

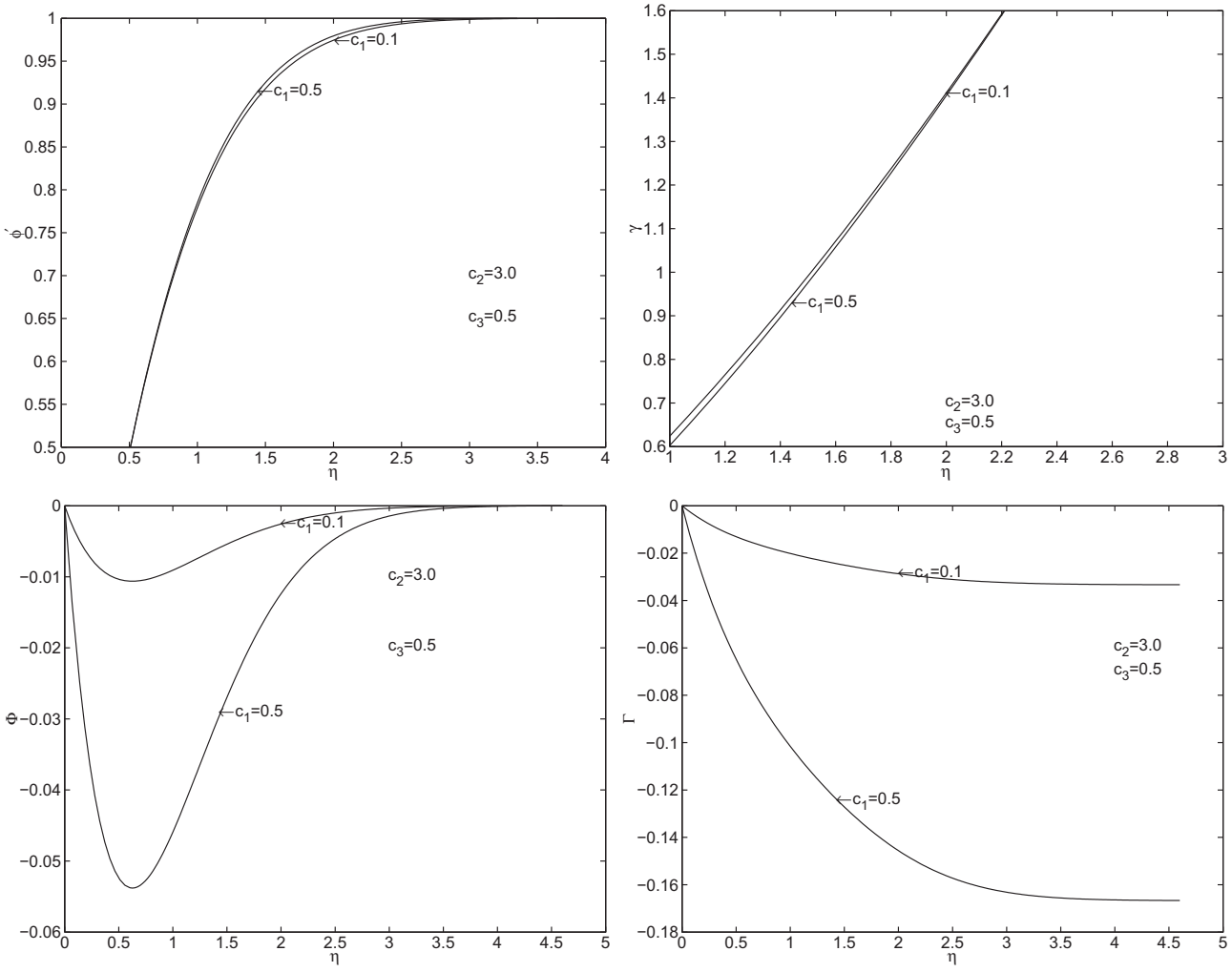

Fig. 9. CASE I-M: plots showing the behaviour of ϕ', γ, Φ and Γ for $c_2 = 3.0$, $c_3 = 0.5$ fixed, and for different values of c_1.

Moreover, the influence of c_1 appears more considerable also on the other quantities quoted in the table.

We have displayed some representative graphs to elucidate the trends of the functions describing the velocities.

In particular, Figs. 4–6 show ϕ,ϕ', ϕ'', Φ, Φ', γ, γ', Γ, Γ' for $c_1 = 0.5$, $c_2 = 3.0$, $c_3 = 0.5$. The other choices of these parameters modify the trends of these functions very slightly.

Of course, the behaviour of ϕ,Φ does not depend on $\beta - \alpha$, unlike γ, Γ.

If we compare the velocity profile with the solution for classical viscous flow [14], we note that the trend is very similar, as was found in [7] for orthogonal stagnation-point flow.

Figs. 7–9 elucidate the dependence of the functions ϕ', γ, Φ, Γ on the parameters c_1, c_2, c_3. We can see that the functions which appear most influenced by c_1, c_2, c_3 are Φ, and Γ – in other words the microrotation. More precisely, the profile of Φ rises as c_3 or c_2 increases and c_1 decreases, while the profile of Γ rises as c_2 increases and c_1 or c_3 decreases. Moreover c_1 is the parameter that most influences the microrotation. The other two functions, ϕ' and γ, do not show considerable variations as c_1, c_2, c_3 assume different values.

Observing $\phi''(0)$, $\gamma'(0)$ in Table 1 we notice that x_s (given by (28)) has the sign of b if $\beta - \alpha > 0$ and the sign of $-b$ if $\beta - \alpha \leqslant 0$. Moreover if b is positive (negative) x_s increases (decreases) as $\beta - \alpha$ increases. As far as $|x_s|$ is concerned, if $\beta - \alpha$ increases from a negative value to zero, $|x_s|$ decreases and so x_s approaches the origin, otherwise, as $\beta - \alpha$ increases from zero to a positive value, $|x_s|$ increases and so x_s departs from the origin. The same results were also found for Newtonian fluids in [14].

Moreover from Table 1 we see that x_p and x_s lie on the same side of the origin, and $\frac{m_s}{m_i}$ is constant once c_1, c_2, c_3 are fixed.

Fig. 10 shows the streamlines and the points

$$\xi_p = \sqrt{\frac{\nu}{a}}x_p, \quad \xi_s = \sqrt{\frac{\nu}{a}}x_s \tag{39}$$

for $\frac{b}{a} = 1$ and $\beta - \alpha = -\alpha$, 0, α, respectively.

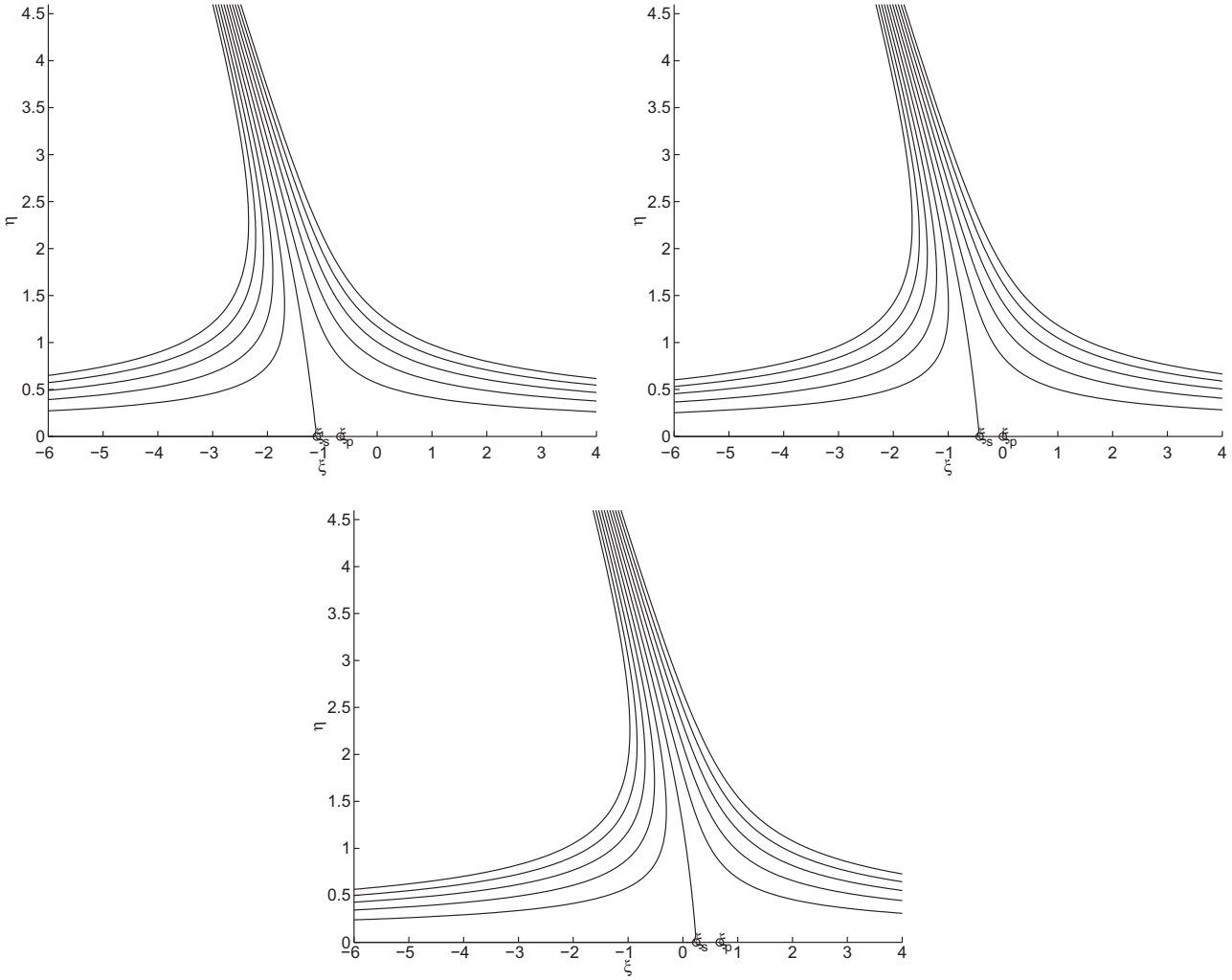

Fig. 10. CASE I-M: plots showing the streamlines and the points ξ_p, ξ_s for $\frac{b}{a} = 1$, $c_1 = 0.5$, $c_2 = 3.0$, $c_3 = 0.5$ and $\beta - \alpha = -\alpha$, 0, α, respectively.

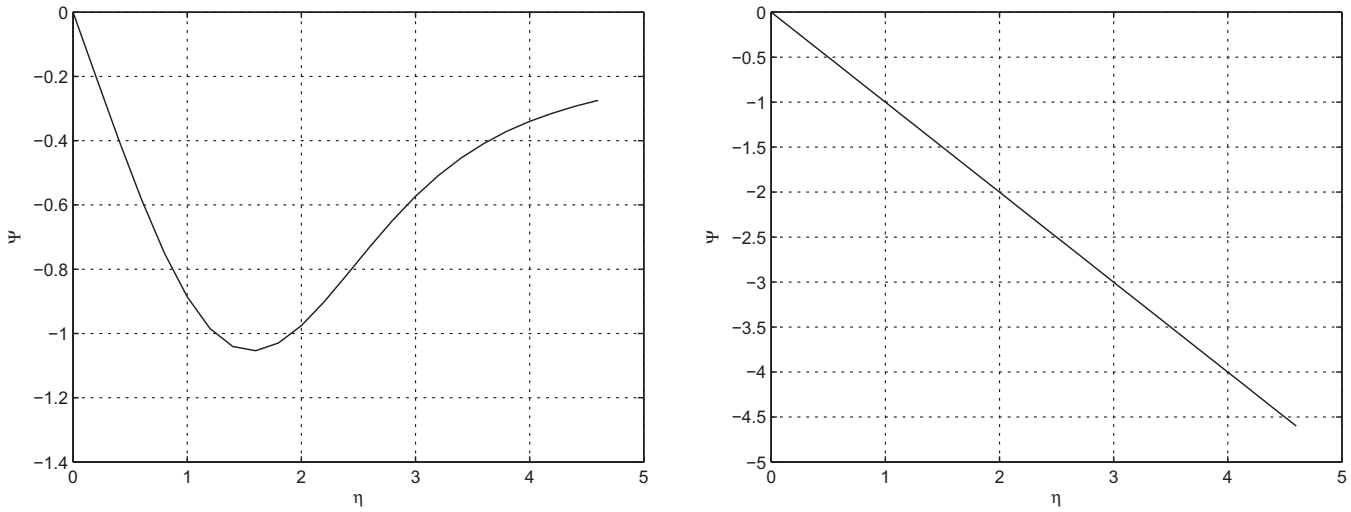

Fig. 11. CASE I-M: plots showing Ψ with $R_m = 1, 10^{-6}$.

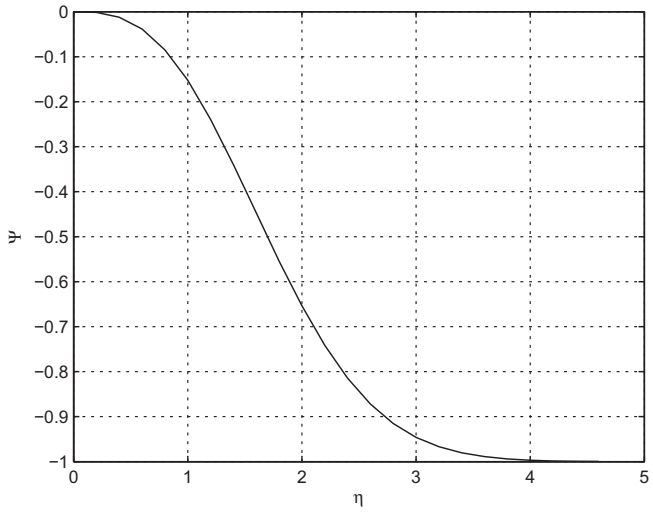

Fig. 12. CASE II-M: plot showing Ψ for $R_m = 1$.

Finally, Fig. 11_1 shows the behaviour of the induced magnetic field Ψ with $R_m = 1$, that is similar to the behaviour of Ψ in CASE I (inviscid fluid), as we can see. Fig. 11_2 shows the behaviour of Ψ with $R_m = 10^{-6}$; for $\eta \in [0,4.6]$ the graph is approximately linear, because in this interval, for very small values of R_m, the Eq. $(31)_3$ reduces to $\Psi' \cong -1$.

4.2. CASE II-M

In this case the ordinary differential problem governing ϕ, γ, Φ, Γ is the same as in (24); we have only to compute $\Psi(\eta)$, given by (33).

Fig. 12 shows that Ψ has a similar behaviour as in CASE II, as we can see.

4.3. CASE III-M

We have solved the problem (38) and (25) with the boundary conditions (25).

Table 2 shows the numerical results of the quantities listed in Table 1 for the same c_1, c_2, c_3, β, choosing $M = 1, 2, 5, 10$.

If we fix M, we see that the considerations of CASE I-M continue to hold.

As far as the dependence on M is concerned, we can see that α and $\Phi'(0)$ decrease and $\phi''(0)$ increases as M is increased from 0, as we would expect physically.

As far as the dependence of $\gamma'(0)$ and $\Gamma'(0)$ on M are concerned, from Table 2 we can see that their values increase as M increases if $\beta - \alpha < 0$, otherwise they decrease.

Table 2
CASE III-M: descriptive quantities of motion for some values of c_1, c_2, c_3 and M.

c_1	c_2	c_3	M	α	$\beta-\alpha$	$\phi''(0)$	$\gamma'(0)$	$\Phi'(0)$	$\Gamma'(0)$	$\frac{x_p}{x_s}$	$\frac{m_s}{m_i}$	$\bar{\eta}_\phi$	$\bar{\eta}_\gamma$
0.1	1.5	0.1	1	0.5386	−0.5386	1.5751	1.3886	−0.0582	−0.0876	0.6110	3.2715	2.3000	2.6833
					0	1.5751	0.5402	−0.0582	−0.0562	0	3.2716	2.3000	2.7259
					0.5386	1.5751	−0.3082	−0.0582	−0.0249	2.7526	3.2716	2.3000	2.8111
			2	0.3924	−0.3924	2.3375	1.4271	−0.0663	−0.0857	0.6426	3.0859	1.6611	2.0444
					0	2.3375	0.5100	−0.0663	−0.0597	0	3.0859	1.6611	2.1722
					0.3924	2.3375	−0.4071	−0.0663	−0.0337	2.2527	3.0859	1.6611	2.1722
			5	0.1905	−0.1905	5.1417	1.4739	−0.0804	−0.0836	0.6646	3.0120	0.9370	1.0222
					0	5.1417	0.4944	−0.0804	−0.0683	0	3.0120	0.9370	1.1074
					0.1905	5.1417	−0.4852	−0.0804	−0.0530	2.0190	3.0120	0.9370	1.1926
			10	0.0987	−0.0987	10.0708	1.4890	−0.0888	−0.0830	0.6678	3.0026	0.4543	0.5537
					0	10.0708	0.4947	−0.0888	−0.0743	0	3.0026	0.4543	0.5963
					0.0987	10.0708	−0.4997	−0.0888	−0.0655	1.9900	3.0026	0.4543	0.6389
		0.5	1	0.5388	−0.5388	1.5762	1.3887	−0.0560	−0.0879	0.6116	3.2702	2.3000	2.6833
					0	1.5762	0.5394	−0.0560	−0.0577	0	3.2702	2.3000	2.7259
					0.5388	1.5762	−0.3098	−0.0560	−0.0275	2.7411	3.2702	2.3000	2.8111
			2	0.3924	−0.3924	2.3383	1.4269	−0.0640	−0.0870	0.6431	3.0853	1.6611	2.0444
					0	2.3383	0.5092	−0.0640	−0.0619	0	3.0853	1.6611	2.1722
					0.3924	2.3383	−0.4084	−0.0640	−0.0368	2.2469	3.0853	1.6611	2.1722
			5	0.1905	−0.1905	5.1421	1.4735	−0.0784	−0.0866	0.6649	3.0119	0.9370	1.0222
					0	5.1421	0.4938	−0.0784	−0.0717	0	3.0119	0.9370	1.1074
					0.1905	5.1421	−0.4859	−0.0784	−0.0567	2.0162	3.0119	0.9370	1.1926
			10	0.0987	−0.0987	10.0710	1.4887	−0.0874	−0.0871	0.6680	3.0026	0.4685	0.5537
					0	10.0710	0.4943	−0.0874	−0.0785	0	3.0026	0.4685	0.5963
					0.0987	10.0710	−0.5001	−0.0874	−0.0698	1.9883	3.0026	0.4685	0.5963
	3.0	0.1	1	0.5392	−0.5392	1.5778	1.4024	−0.0497	−0.0642	0.6066	3.2902	2.3000	2.6833
					0	1.5778	0.5517	−0.0497	−0.0374	0	3.2902	2.3000	2.8111
					0.5392	1.5778	−0.2990	−0.0497	−0.0106	2.8451	3.2902	2.3000	2.9389
			2	0.3926	−0.3926	2.3395	1.4370	−0.0584	−0.0622	0.6392	3.0932	1.6611	2.0444
					0	2.3395	0.5185	−0.0584	−0.0393	0	3.0932	1.6611	2.1722
					0.3926	2.3395	−0.4000	−0.0584	−0.0163	2.2964	3.0932	1.6611	2.3000
			5	0.1905	−0.1905	5.1426	1.4787	−0.0748	−0.0596	0.6627	3.0132	0.9370	1.0222
					0	5.1426	0.4988	−0.0748	−0.0453	0	3.0132	0.9370	1.1074
					0.1905	5.1426	−0.4810	−0.0748	−0.0311	2.0369	3.0132	0.9370	1.1926
			10	0.0987	−0.0987	10.0711	1.4915	−0.0851	−0.0586	0.6667	3.0028	0.4685	0.5537
					0	10.0711	0.4971	−0.0851	−0.0502	0	3.0028	0.4685	0.5963
					0.0987	10.0711	−0.4974	−0.0851	−0.0418	1.9994	3.0028	0.4685	0.6389
		0.5	1	0.5392	−0.5392	1.5783	1.4027	−0.0487	−0.0638	0.6068	3.2902	2.3000	2.6833
					0	1.5783	0.5516	−0.0487	−0.0376	0	3.2902	2.3000	2.8111
					0.5392	1.5783	−0.2995	−0.0487	−0.0114	2.8417	3.2902	2.3000	2.9389
			2	0.3927	−0.3927	2.3399	1.4372	−0.0572	−0.0622	0.6393	3.0932	1.6611	2.0444
					0	2.3399	0.5184	−0.0572	−0.0397	0	3.0931	1.6611	2.1722
					0.3927	2.3399	−0.4004	−0.0572	−0.0173	2.2947	3.0931	1.6611	2.3000
			5	0.1905	−0.1905	5.1428	1.4786	−0.0736	−0.0603	0.6627	3.0131	0.9370	1.0222
					0	5.1428	0.4987	−0.0736	−0.0463	0	3.0131	0.9370	1.1074
					0.1905	5.1428	−0.4813	−0.0736	−0.0323	2.0361	3.0131	0.9370	1.1926
			10	0.0987	−0.0987	10.0712	1.4914	−0.0842	−0.0598	0.6668	3.0028	0.4685	0.5537
					0	10.0712	0.4969	−0.0842	−0.0515	0	3.0028	0.4685	0.5963
					0.0987	10.0712	−0.4975	−0.0842	−0.0432	1.9989	3.0028	0.4685	0.6389
0.5	1.5	0.1	1	0.5290	−0.5290	1.5335	1.2465	−0.2913	−0.4247	0.6508	3.0440	2.0444	2.3000
					0	1.5335	0.4353	−0.2913	−0.2706	0	3.0442	2.0444	2.4278
					0.5290	1.5335	−0.3760	−0.2913	−0.1165	2.1577	3.0443	2.0444	2.4278
			2	0.3874	−0.3874	2.3005	1.3193	−0.3315	−0.4208	0.6755	2.9716	1.5333	1.6611
					0	2.3005	0.4281	−0.3315	−0.2924	0	2.9716	1.5333	1.9167
					0.3874	2.3005	−0.4630	−0.3315	−0.1639	1.9246	2.9716	1.5333	1.9167
			5	0.1896	−0.1896	5.1166	1.4170	−0.4022	−0.4159	0.6847	2.9810	0.8519	0.9370
					0	5.1166	0.4467	−0.4022	−0.3396	0.0000	2.9810	0.8519	1.0222
					0.1896	5.1166	−0.5236	−0.4022	−0.2634	1.8533	2.9810	0.8519	1.1074
			10	0.0986	−0.0986	10.0552	1.4581	−0.4440	−0.4145	0.6798	2.9931	0.4543	0.5111
					0	10.0552	0.4668	−0.4440	−0.3707	0	2.9931	0.4543	0.5537
					0.0986	10.0552	−0.5245	−0.4440	−0.3270	1.8901	2.9930	0.4543	0.5963
		0.5	1	0.5299	−0.5299	1.5392	1.2469	−0.2802	−0.4267	0.6541	3.0373	2.0444	2.1722
					0	1.5392	0.4313	−0.2802	−0.2783	0.0000	3.0373	2.0444	2.4278
					0.5299	1.5392	−0.3843	−0.2802	−0.1298	2.1222	3.0373	2.0444	2.4278
			2	0.3878	−0.3878	2.3048	1.3181	−0.3199	−0.4272	0.6781	2.9686	1.6611	1.6611
					0	2.3048	0.4242	−0.3199	−0.3031	0	2.9686	1.6611	1.7889
					0.3878	2.3048	−0.4696	−0.3199	−0.1790	1.9033	2.9686	1.6611	1.9167

(*continued on next page*)

Table 2 (*continued*)

c_1	c_2	c_3	M	α	$\beta-\alpha$	$\phi''(0)$	$\gamma'(0)$	$\Phi'(0)$	$\Gamma'(0)$	$\frac{x_p}{x_s}$	$\frac{m_s}{m_i}$	$\bar{\eta}_\phi$	$\bar{\eta}_\gamma$
			5	0.1897	−0.1897	5.1184	1.4146	−0.3921	−0.4307	0.6864	2.9802	0.8519	0.9370
					0	5.1184	0.4437	−0.3921	−0.3563	0	2.9802	0.8519	1.0222
					0.1897	5.1184	−0.5272	−0.3921	−0.2819	1.8416	2.9802	0.8519	1.1074
			10	0.0986	−0.0986	10.0559	1.4562	−0.4368	−0.4347	0.6808	2.9929	0.4685	0.5111
					0	10.0559	0.4648	−0.4368	−0.3916	0	2.9929	0.4685	0.5537
					0.0986	10.0559	−0.5266	−0.4368	−0.3486	1.8826	2.9929	0.4685	0.5963
	3.0		1	0.5317	−0.5317	1.5475	1.3160	−0.2487	−0.3140	0.6253	3.1370	2.0444	2.5556
					0	1.5475	0.4931	−0.2487	−0.1818	0	3.1371	2.0444	2.5556
					0.5317	1.5475	−0.3297	−0.2487	−0.0496	2.4958	3.1371	2.0444	2.7259
			2	0.3886	−0.3886	2.3108	1.3689	−0.2922	−0.3066	0.6560	3.0081	1.6611	1.9167
					0	2.3108	0.4708	−0.2922	−0.1930	0	3.0081	1.6611	2.0444
					0.3886	2.3108	−0.4272	−0.2922	−0.0795	2.1021	3.0081	1.6611	2.0444
			5	0.1898	−0.1898	5.1209	1.4407	−0.3738	−0.2965	0.6746	2.9867	0.8519	0.9370
					0	5.1209	0.4689	−0.3738	−0.2255	0	2.9867	0.8519	1.0222
					0.1898	5.1209	−0.5030	−0.3738	−0.1546	1.9322	2.9867	0.8519	1.1074
			10	0.0986	−0.0986	10.0568	1.4703	−0.4257	−0.2926	0.6744	2.9941	0.4685	0.5111
					0	10.0568	0.4787	−0.4257	−0.2506	0	2.9941	0.4685	0.5537
					0.0986	10.0568	−0.5129	−0.4257	−0.2086	1.9335	2.9941	0.4685	0.5963
		0.5	1	0.5321	−0.5321	1.5501	1.3175	−0.2434	−0.3124	0.6261	3.1373	2.0444	2.5556
					0	1.5501	0.4926	−0.2434	−0.1829	0	3.1373	2.0444	2.7259
					0.5321	1.5501	−0.3323	−0.2434	−0.0534	2.4827	3.1373	2.0444	2.7259
			2	0.3889	−0.3889	2.3129	1.3696	−0.2862	−0.3066	0.6567	3.0078	1.6611	1.9167
					0	2.3129	0.4701	−0.2862	−0.1953	0	3.0078	1.6611	2.0444
					0.3889	2.3129	−0.4293	−0.2862	−0.0840	2.0951	3.0078	1.6611	2.0444
			5	0.1898	−0.1898	5.1219	1.4403	−0.3678	−0.3000	0.6750	2.9864	0.8519	0.9370
					0	5.1219	0.4681	−0.3678	−0.2302	0	2.9864	0.8519	1.0222
					0.1898	5.1219	−0.5041	−0.3678	−0.1604	1.9284	2.9864	0.8519	1.1074
			10	0.0986	−0.0986	10.0572	1.4698	10.0572	−0.2986	0.6747	2.9940	0.4685	0.5111
					0	10.0572	0.4781	10.0572	−0.2571	0	2.9940	0.4685	0.5537
					0.0986	10.0572	−0.5136	10.0572	−0.2156	1.9310	2.9940	0.4685	0.5963

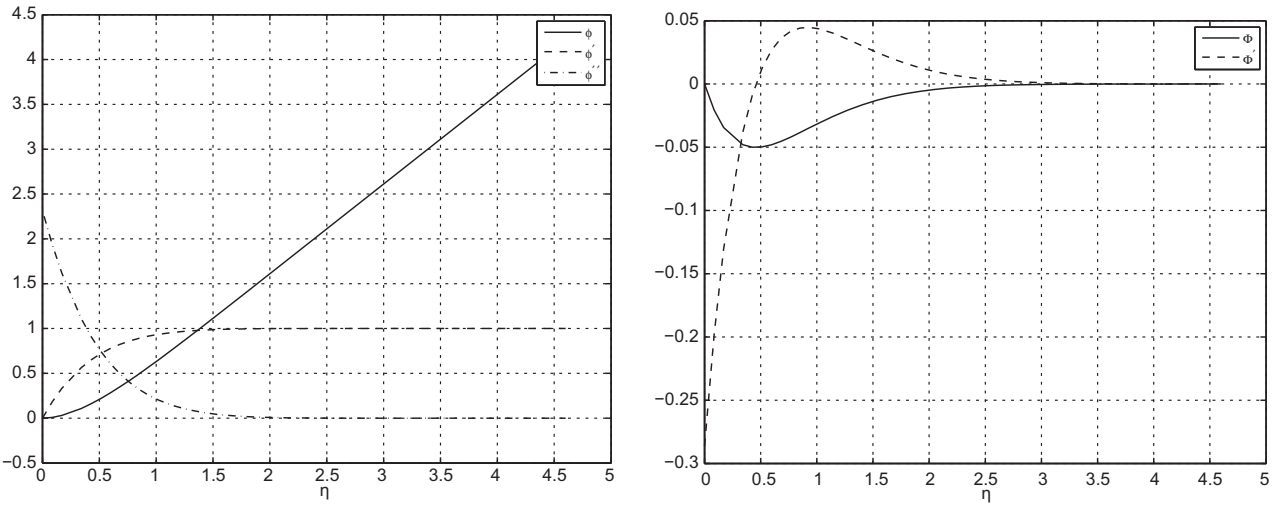

Fig. 13. CASE III-M: plots showing ϕ, ϕ', ϕ'' and Φ, Φ' (respectively) for $c_1 = 0.5$, $c_2 = 3.0$, $c_3 = 0.5$ and $M = 2$.

In Fig. 13$_1$, we have plotted the profiles ϕ, ϕ', ϕ'' for $M = 2$ and $c_1 = 0.5$, $c_2 = 3.0$, $c_3 = 0.5$, while Fig. 16 shows the behaviour of ϕ' for different M and the same values of c_1, c_2, c_3.

Fig. 14$_1$, Fig. 14$_2$ show the profiles of $\gamma(\eta)$, $\gamma'(\eta)$, for $M = 2$, $c_1 = 0.5$, $c_2 = 3.0$, $c_3 = 0.5$ and for some values of $\beta - \alpha$, i.e. $\beta - \alpha = -\alpha$, 0, α. In Figs. 17 and 18, we provide the behaviour of γ' for different M when $c_1 = 0.5$, $c_2 = 3.0$, $c_3 = 0.5$ and $\beta - \alpha$ is fixed.

In Fig. 13$_2$, we can see the profiles Φ, Φ' for $M = 2$ and $c_1 = 0.5$,$c_2 = 3.0$, $c_3 = 0.5$.

Fig. 15$_1$, Fig. 15$_2$ show the graphics of $\Gamma(\eta)$, $\Gamma'(\eta)$, for $M = 2$, $c_1 = 0.5$, $c_2 = 3.0$, $c_3 = 0.5$ and for some values of $\beta - \alpha$, i.e. $\beta - \alpha = -\alpha$, 0, α.

We have only plotted the profiles of ϕ, ϕ', ϕ'', γ, γ', Φ, Φ', Γ, Γ' for $M = 2$ and $c_1 = 0.5$, $c_2 = 3.0$, $c_3 = 0.5$, because they have an analogous behaviour for $M \neq 2$ and different c_1, c_2, c_3.

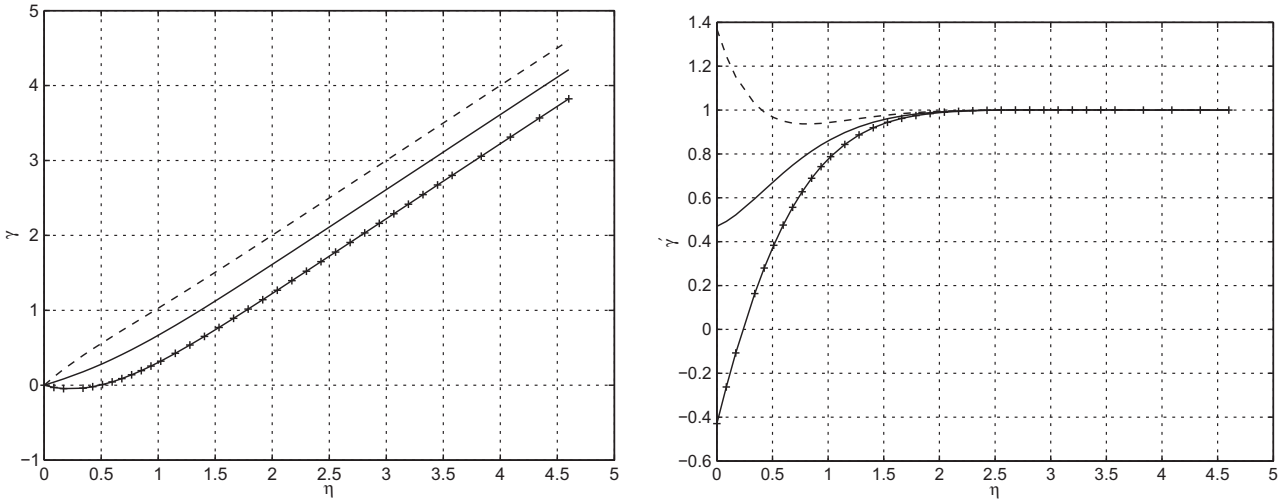

Fig. 14. CASE III-M: plots showing γ, γ' with $M = 2$, $c_1 = 0.5$, $c_2 = 3.0$, $c_3 = 0.5$ and, from above, $\beta - \alpha = -\alpha$, 0, α, respectively.

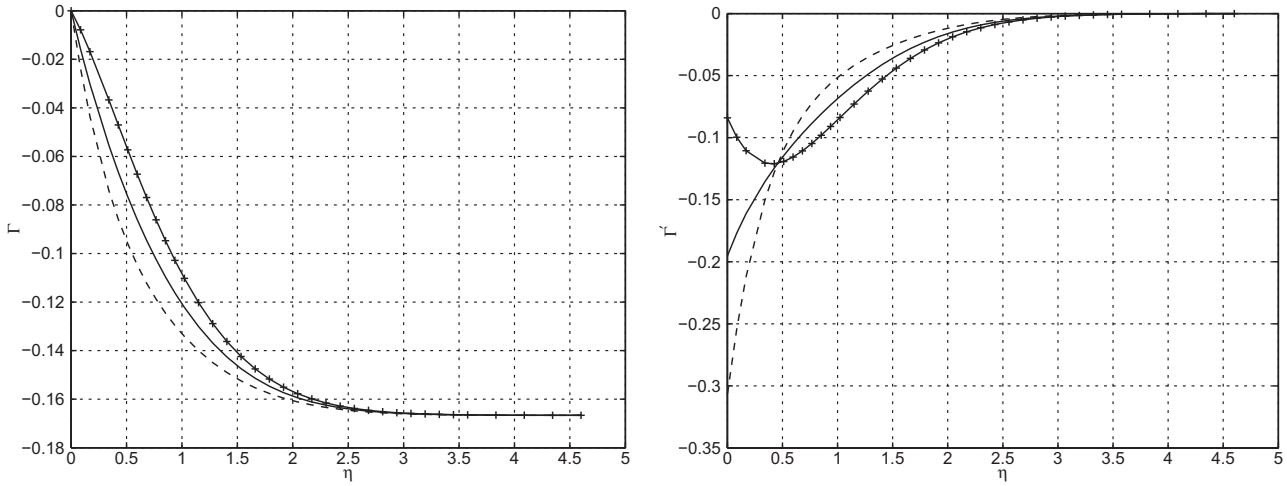

Fig. 15. CASE III-M: plots showing Γ, Γ' with $M = 2$, $c_1 = 0.5$, $c_2 = 3.0$, $c_3 = 0.5$ and, from above, $\beta - \alpha = -\alpha$, 0, α, respectively.

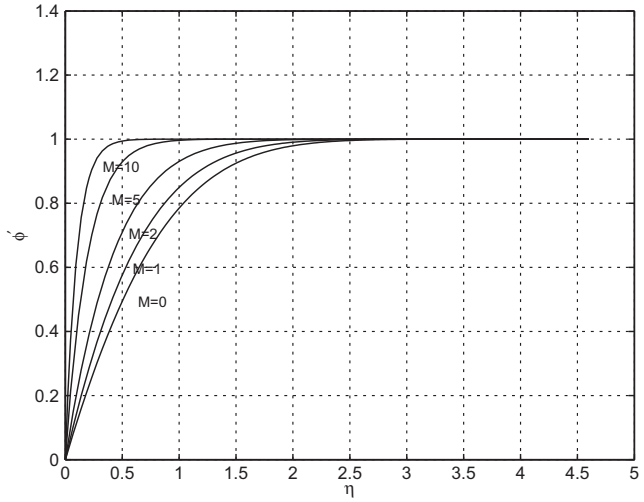

Fig. 16. CASE III-M: plots showing ϕ' with $c_1 = 0.5$, $c_2 = 3.0$, $c_3 = 0.5$ and for different M.

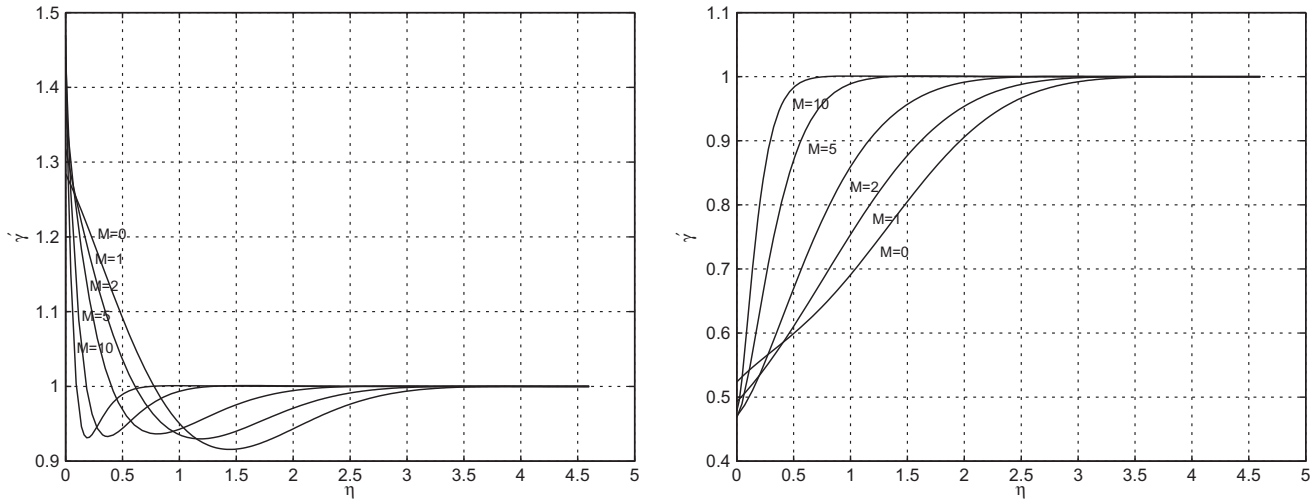

Fig. 17. CASE III-M: plots showing γ' with $c_1 = 0.5$, $c_2 = 3.0$, $c_3 = 0.5$ and for different M. In the first picture $\beta - \alpha = -\alpha$, in the second $\beta - \alpha = 0$.

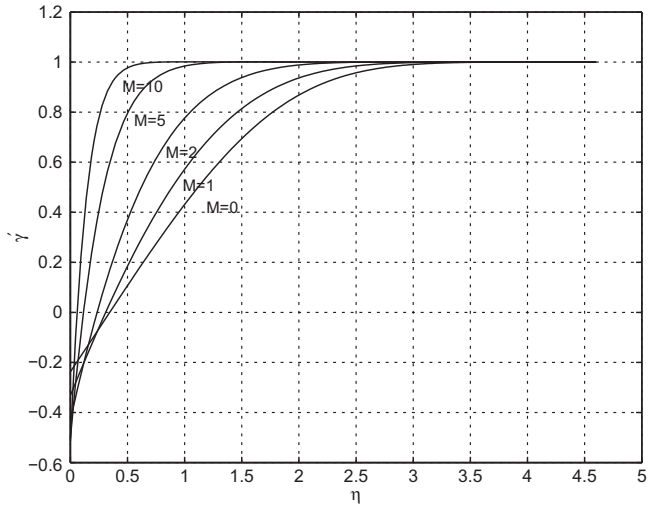

Fig. 18. CASE III-M: plot showing γ' with $c_1 = 0.5$, $c_2 = 3.0$, $c_3 = 0.5$, $\beta - \alpha = \alpha$ and for different M.

In Table 2, we also list the values of $\bar{\eta}_\phi, \bar{\eta}_\gamma$ beyond which $\phi = \eta - \alpha$ and $\gamma = \eta - \beta$, respectively. We note that $\bar{\eta}_\gamma$ is greater than the corresponding value of $\bar{\eta}_\phi$; so the influence of the viscosity appears only in the region $\eta < \bar{\eta}_\gamma$, i.e. $x_2 < \sqrt{\frac{\nu + \nu_r}{a}}\bar{\eta}_\gamma$. Further we underline that the thickness of this layer depends on M and it decreases as M increases (as easily seen in Figs. 16–18). This effect is normal in magnetohydrodynamics.

Finally, we notice that the points x_p, x_s, given by (27) and by (28), lie on the same side of the origin. Their location depends on M, c_1, c_2, c_3 and $\beta - \alpha$, as seen in Table 2. The Fig. 19 shows the streamlines and the points ξ_p, ξ_s for $\frac{b}{a} = 1,\ c_1 = 0.5,\ c_2 = 3.0,\ c_3 = 0.5,\ \beta - \alpha = -\alpha, 0, \alpha$, and $M = 1, 5$.

5. Conclusions

In this article, the analysis was carried out for the MHD oblique stagnation-point flow of an electrically conducting micropolar fluid. The main advantage of using a micropolar fluid model to study this problem in comparison with other classes of non-Newtonian fluids is that it takes into account the rotation of fluid particles by means of an independent kinematic vector called the micro-rotation vector. This model is considered to describe, for example, biological fluids in thin vessels, polymeric suspensions, slurries, colloidal fluids.

The aim of the work presented above was to study how the flow is influenced by a uniform external electromagnetic field. The results are original and should be useful in our understanding of MHD flows near stagnation regions.

We have analysed three significant physical situations.

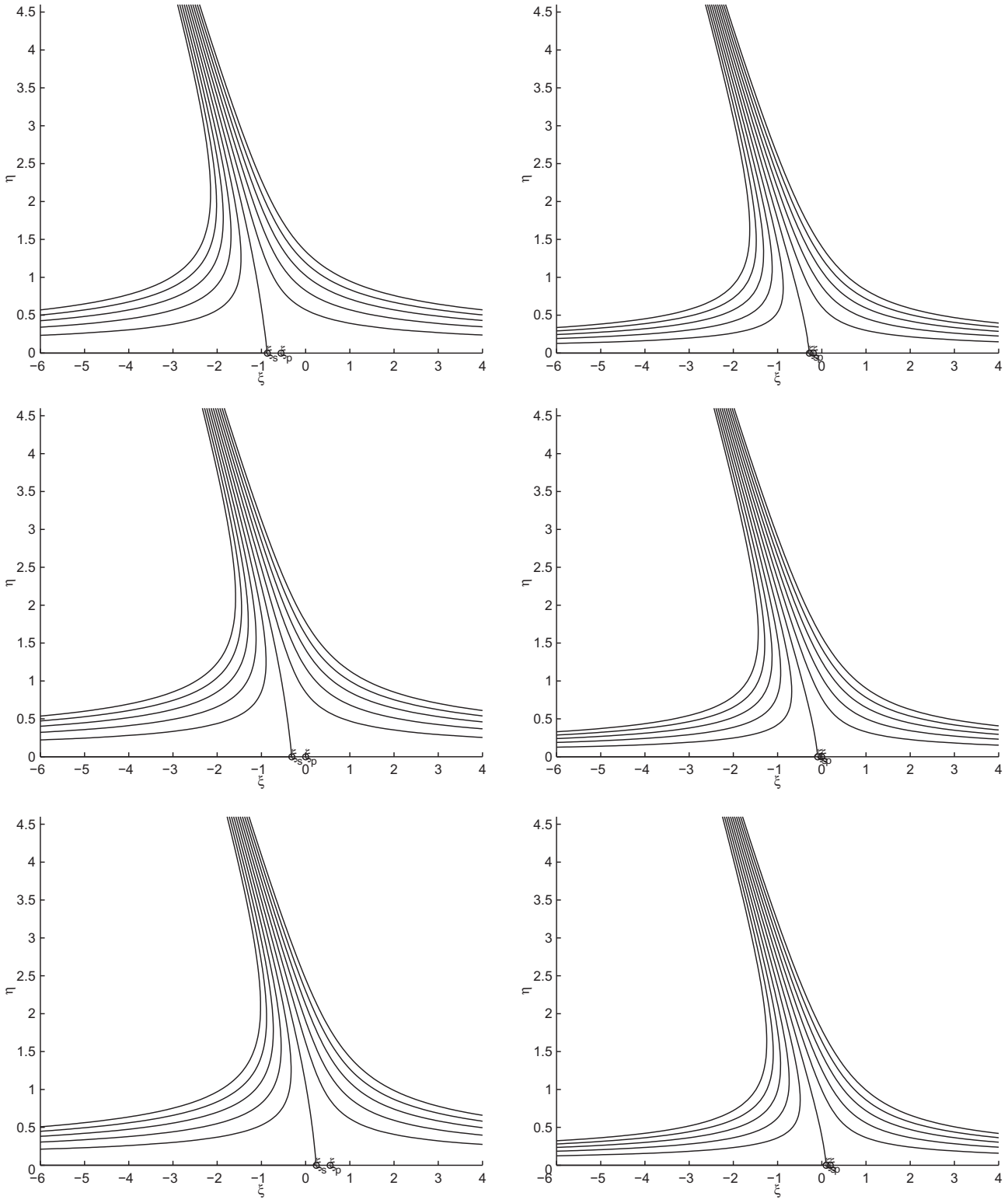

Fig. 19. CASE III-M: Fig. $19_{1,3,5}$ show the streamlines and the points ξ_p, ξ_s for $\frac{b}{a} = 1,\ c_1 = 0.5,\ c_2 = 3.0,\ c_3 = 0.5$ and $\beta - \alpha = -\alpha, 0, \alpha$, respectively and $M = 1$. Fig. $19_{2,4,6}$ for $M = 5$.

In the first two cases, an external constant field, either electric or magnetic ($\mathbf{E}_0$ or $\mathbf{H}_0$), is impressed parallel to the rigid wall. In both cases, we have determined the exact induced magnetic field and we have found that the velocity is not modified by the presence of the external field.

In the third case, if $\mathbf{E}_0$ vanishes, $\mathbf{H}_0$ lies in the plane of the flow, with a direction not parallel to the boundary, and the induced magnetic field is neglected, we have proved that the oblique stagnation-point flow exists if, and only if, the external magnetic field is parallel to the dividing streamline. Moreover we have found that the flow has to satisfy an ordinary

differential problem whose solution depend on $\mathbf{H}_0$ through the Hartmann number M. Further, when the material parameters are fixed, the influence of the viscosity appears only in a layer near to the wall depending on M whose thickness decreases as M increases from zero.

The reduced system of ordinary differential equations was numerically solved using the MATLAB finite difference code **bvp4c**.

The results of velocity and microrotation were plotted and the effects of the presence of the external electromagnetic field were discussed.

As far as applications are concerned, from a theoretical point of view, flows of this type are fundamental in fluid dynamics.

From a practical point of view, it may be noticed that stagnation-point flows are ubiquitous in the sense that they inevitably appear as a component of more complicated flow fields. So the investigation in this area is motivated by the possibility of solving exactly the boundary layer equations at the stagnation point and by their relevance to a wide range of engineering, industrial and technical applications such as cooling of electronic devices by fans, cooling of nuclear reactors during emergency shutdown, solar central receivers exposed to wind currents, and many hydrodynamic process.

Finally, it should be pointed out that a number of aspects of this problem should be further investigated. In particular, the consideration of temperature or time dependance.

References

[1] A.C. Eringen, Theory of micropolar fluids, J. Math. Mech. 16 (1966) 1–18.
[2] A.C. Eringen, Microcontinuum Field Theories, vol. I–II, Springer-Verlag, 2001.
[3] G. Lukaszewicz, Micropolar Fluids Theory and Applications, Birkäuser, 1999.
[4] J.T. Stuart, The viscous flow near a stagnation point when the external flow has uniform vorticity, J. Aerospace Sci. 26 (1959) 124–125.
[5] C.Y. Wang, Similarity stagnation point solutions of the Navier–Stokes equations-review and extension, Eur. J. Mech. B-Fluids 27 (2008) 678–683.
[6] P. Drazin, N. Riley, The Navier–Stokes Equations, in: A Classification of Flows and Exact Solutions, London Mathematical Society, Lecture Notes Series, vol. 334, Cambridge University Press, 2007.
[7] G.S. Guram, A.C. Smith, Stagnation flows of micropolar fluids with strong and weak interactions, Comput. Math. Appl. 6 (1980) 213–233.
[8] G. Ahmadi, Self-Similar solution of incompressible micropolar boundary layer flow over a semi-infinite plate, Int. F. Eng. Sci. 10 (1976) 639–646.
[9] Y.Y. Lok, I. Pop, A.J. Chamkha, Non-orthogonal stagnation-point flow of a micropolar fluid, Int. J. Eng. Sci. 45 (2007) 173–184.
[10] Y.Y. Lok, I. Pop, D.B. Ingham, Oblique stagnation slip flow of a micropolar fluid, Meccanica 45 (2010) 187–198.
[11] T. Hayat, T. Javed, Z. Abbas, MHD flow of a micropolar fluid near a stagnation-point towards a non-linear stretching surface, Nonlinear Anal. Real World Appl. 10 (2009) 15141526.
[12] T. Hayat, T. Javed, Z. Abbas, Corrigendum to "MHD flow of a micropolar fluid near a stagnation-point towards a non-linear stretching surface", Nonlinear Anal. Real World Appl. 11 (2010) 2190.
[13] A. Ishak, R. Nazar, I. Pop, Magnetohydrodynamic (MHD) flow of a micropolar fluid towards a stagnation point on a vertical surface, Comput. Math. Appl. 56 (2008) 3188–3194.
[14] A. Borrelli, G. Giantesio, M.C. Patria, MHD oblique stagnation-point flow of a Newtonian fluid, ZAMP, in press.
[15] R.M. Tooke, M.G. Blyth, A note on oblique stagnation-point flow, Phys. Fluids 20 (2008) 1–3.
[16] C. Pozrikidis, Introduction to Theoretical and Computational Fluid Dynamics, Oxford University Press, 1997.
[17] H. Schlichting, K. Gersten, Boundary Layer Theory, eighth revised and enlarged ed., Springer, 2003.
[18] L.F. Shampine, I. Gladwell, S. Thompson, Solving ODEs with MATLAB, Cambridge University Press, 2003.
[19] J.M. Dorrepaal, Is two-dimensional oblique stagnation-point flow unique?, Can Appl. Math. Q. 8 (2000) 61–66.